Role and mechanism of mitochondrial dysfunction-related gene biomarkers in the progression of type 2 diabetes mellitus

MENGXUE LIU[1,2] and HONG QIAO[1]

[1]Department of Endocrinology and Metabolism, The Second Affiliated Hospital of Harbin Medical University, Harbin, Heilongjiang 150086, P.R. China; [2]Department of Endocrinology, The Fourth Hospital of Harbin, Harbin, Heilongjiang 150026, P.R. China

Received October 17, 2024; Accepted February 19, 2025

DOI: 10.3892/mmr.2025.13523

Abstract. The present study aimed to elucidate the roles and mechanisms of gene biomarkers associated with mitochondrial dysfunction in the progression of Type 2 diabetes mellitus (T2DM). It conducted an analysis of differentially expressed genes related to mitochondrial dysfunction in T2DM and employed bioinformatics approaches to predict potential target drugs for key biomarkers. Additionally, the present study used the EPIC algorithm to examine immune cell infiltration in T2DM. Furthermore, the single-cell RNA sequencing dataset GSE221156 was analyzed to identify specific cell types involved in T2DM. The expression of biomarkers was investigated through cellular experiments to assess the effect of marker genes on macrophage polarization. A total of five biomarker genes associated with T2DM were identified, namely ERAP2, HLA-DQB1, HLA-DRB5, MAP1B and OAS3. The combined detection of these genes yielded a risk-predictive area under the curve value of 0.833 for T2DM. These five marker genes may serve as potential targets for valproic acid (VPA). During the progression of T2DM, there is an increase in macrophage numbers, with these genes being highly expressed in macrophages. In a high glucose-induced RAW264.7 macrophage model, the expressions of MAP1B and OAS3 were upregulated. Notably, the knockdown of OAS3 markedly reduced M1 macrophage polarization, indicating OAS3 facilitates M1 macrophage polarization in a high-glucose environment. The downregulation of OAS3 expression attenuated M1 macrophage polarization by inhibiting mTORC activation. In conclusion, five candidate biomarkers for T2DM were identified that may serve as therapeutic targets for VPA and are associated with immune infiltration in T2DM. Among these, OAS3 enhances M1 macrophage polarization in a high-glucose environment by regulating the mTORC1 pathway.

Correspondence to: Dr Hong Qiao, Department of Endocrinology and Metabolism, The Second Affiliated Hospital of Harbin Medical University, 246 Xuefu Road, Nangang, Harbin, Heilongjiang 150086, P.R. China
E-mail: qiaohong@hrbmu.edu.cn

Key words: type 2 diabetes, mitochondrial dysfunction, OAS3, macrophage polarization, valproic acid

Introduction

Diabetes mellitus (DM) is a chronic metabolic disease characterized by persistent hyperglycemia and is divided into two predominant subtypes: type 2 diabetes mellitus (T2DM) and type 1 diabetes mellitus (T1DM) (1). DM is a serious threat to human health globally and it is estimated that there are currently 537 million adults with DM worldwide (2). The number of individuals with DM diabetes will increase to 643 million by 2030, with T2DM accounting for more than 90% of these cases (2). T2DM is a polygenic genetic disease caused by genetic and environmental factors, with insulin resistance and defective insulin secretion from β-cells as the two main pathologic mechanisms (3,4). A previous study demonstrated that patients with T2DM are in a state of long-term high blood sugar, which can induce heart, brain, kidney and other target organ damage, thus leading to a variety of complications and seriously endangering the lives of patients (4). Studies have observed that weight loss through bariatric surgery, aggressive insulin therapy and behavioral interventions can lead to sustained remission of T2DM for several years; most T2DM patients require continuous treatment to maintain glycemic compliance (5,6). In addition, there are several drugs (alpha-glucosidase inhibitors, metformin, sulfonylureas and meglitinides) that have adverse effects in the current treatment of T2DM, for example, sulfonylureas can lead to decreased efficacy and hypoglycemia and metformin may trigger intestinal discomfort in patients (7). Early diagnosis and intervention in T2DM, facilitated by a thorough understanding of its onset and progression mechanisms, can substantially improve patient quality of life and effectively reduce the risk of complications. This approach constitutes an essential aspect of comprehensive diabetes management. Nevertheless, existing screening and monitoring methodologies, such as fasting blood glucose and glycosylated hemoglobin (HbA1c) testing, are insufficient and necessitate further refinement (8).

Emerging biomarkers, including glycated albumin, fructosamine and 1,5-anhydroglucitol (1,5-AG), have shown enhanced prognostic value over traditional markers, offering a more accurate assessment of blood glucose levels (8). A

previous study revealed that T2DM is characterized by low adenosine triphosphate (ATP) levels, high reactive oxygen species (ROS) production and mitochondrial dysfunction (9). Mitochondria are bioenergetic and metabolic centers extensively involved in various biological processes with complex adaptive mechanisms (10). Alterations in the normal morphology and dysfunction of mitochondria are relevant factor pairs affecting the progression of multiple diseases (11). A number of researchers have identified mitochondria as the intersection of key cellular pathways such as ROS generation, energy substrate metabolism and apoptosis in T2DM and mitochondria contribute to deficits in important functions downstream of T2DM, including cardiac output, hepatocyte metabolism, skeletal muscle contraction, neuronal health and β-cell insulin production (12). Within mitochondria, the catabolism of carbohydrates and fatty acids results in the generation of ATP and ROS (13). Under physiological conditions, mitochondria regulate ROS concentrations via intrinsic antioxidant systems. However, in the context of T2DM, mitochondrial functionality is compromised and energy metabolism is disrupted, culminating in elevated ROS production (14). Mitophagy, a form of selective autophagy, regulates the progression of T2DM by specifically degrading dysfunctional or damaged mitochondria (15). Therefore, the present study conducted a screening of endoplasmic reticulum aminopeptidase 2 (ERAP2), human leukocyte antigen (HLA)-DQB1, HLA-DRB5, microtubule-associated protein 1B (MAP1B) and 2'-5'-oligoadenylate synthetases 3 (OAS3) as potential biomarkers and therapeutic targets for T2DM. This screening was based on the expression levels of genes associated with mitochondrial dysfunction in T2DM.

In addition to metabolic disturbances, an imbalance in immune homeostasis is a key feature of T2DM and can lead to increased inflammatory infiltration (16). Using bioinformatics analysis, it was identified that the aforementioned five biomarkers-ERAP2, HLA-DQB1, HLA-DRB5, MAP1B and OAS3 are all highly expressed in macrophages. Macrophages are the main cells that carry out the body's intrinsic immunity and activated macrophages participate in the inflammatory response by releasing a variety of cytokines and inflammatory mediators (17). Different phenotypes of macrophages have great differences in inflammatory reactions. They can be divided into pro-inflammatory M1 macrophages and anti-inflammatory M2 macrophages and the M1 and M2 types of macrophages can be transformed into each other under appropriate conditions (17). The microenvironment of DM patients is in a state of inflammation. The imbalance of macrophage M1/M2 polarization is associated with insulin resistance and pancreatic islet β-cell damage and the adjustment of macrophage polarization plays a therapeutic role in T2DM (17).

The present study established a 5-gene (ERAP2, HLA-DQB1, HLA-DRB5, MAP1B and OAS3) prediction model for T2DM prediction and analyzed the association of marker genes with the immune microenvironment. In addition, the association of MAP1B and OAS3 with macrophages during T2DM pathology was explored by cellular experiments. The present study aided in the early diagnosis, prevention and treatment of T2DM.

Materials and methods

Data collection and processing. In the present study, the gene expression dataset GSE184050, associated with T2DM and the single-cell transcriptomics dataset GSE221156, associated with T2DM, were downloaded from the Gene Expression Omnibus (GEO) database (https://www.ncbi.nlm.nih.gov/geo/). The GSE184050 dataset includes sequencing results of peripheral blood samples from 50 patients with T2DM and 66 controls. The GSE221156 dataset includes sequencing results of pancreatic single-cell suspensions from 17 patients with T2DM, 17 control populations and 14 patients with pre-diabetes (prediabetic state; PD). A total of 9,189 mitochondrial dysfunction-related genes were downloaded from the GeneCard database (https://www.genecards.org/) using the keyword 'mitochondrial dysfunction'.

The expression matrix of T2DM-related genes was extracted from the GSE184050 dataset using the R package 'limma' (version 3.2.0; https://www.bioconductor.org/packages/release/bioc/html/limma.html) and analyzed by differential expression and the cut-off criterion for differentially expressed genes (DEGs) was set at FC=1.3, P<0.05; volcano plots showed the final results. The R package 'WGCNA' (version 1.73; https://cran.r-project.org/web/packages/WGCNA/index.html) was applied to construct and visualize the network of genes in the GSE184050 dataset. First, the outliers were identified and removed by the sample clustering method and feature matching was performed.

Based on the 9,189 mitochondrial dysfunction-related genes, DEGs screened in the GSE184050 dataset and important modular genes obtained by WGCNA, the intersection analysis was further carried out by using the 'VennDiagram' R package (version 1.7.3; https://cran.r-project.org/web/packages/VennDiagram/index.html) and key genes related to mitochondrial dysfunction in T2DM in the present study were identified through the Venn diagram.

T2DM-related single-cell transcriptome data (GSE221156 dataset) were analyzed using the 'Seurat' R package (version 5.2.1; https://cran.r-project.org/web/packages/Seurat/index.html) to identify and annotate cell types and their subpopulations.

T2DM-related differential gene analysis and co-expression module construction. Weighted gene co-expression network analysis (WGCNA) is an algorithm developed based on the R language, which is mainly used to mine valuable information in high-throughput data. WGCNA identifies core genes associated with diseases in scale-free networks through clustering analysis and thus helps to reveal complex biological mechanisms (18). The network construction was performed on the genes in the GSE184050 dataset. The Pearson correlation coefficient was used to obtain the gene co-expression similarity. Then, the topological overlap matrix was used to filter the weak connections in the network construction process. When the soft threshold was set to five, the constructed network conformed to the scale-free distribution and provided appropriate average connections for the subsequent co-expression module building. Finally, the branches of the dendrogram were efficiently identified using the dynamic tree-cutting algorithm, thus defining different

co-expression modules and representing them differentially with other colors. Correlation tests were performed on gene modules using Pearson correlation analysis to explore the relationships between gene modules further.

In addition, the present study screened modules closely associated with T2DM by constructing module-trait correlations. In this process, gene significance was defined by the association values between specific traits and gene expression within a module; Module eigengene and Module membership were used to differentiate significant modules associated with T2DM. Finally, modules with P<0.05 were selected for subsequent in-depth analysis.

Key gene screening and functional enrichment analysis. Next, the present study performed functional enrichment analysis on the screened key genes. Gene Ontology (GO) and the Kyoto Encyclopedia of Genes and Genomes (KEGG) can be used to identify key biological pathways. The present study performed GO annotation and KEGG pathway enrichment analysis of key genes using the R packages 'org.Hs.eg.db' (version 3.20; https://bioconductor.org/packages/release/data/annotation/html/org.Hs.eg.db.html) and 'clusterProfiler' (version 3.20; https://www.bioconductor.org/packages/release/bioc/html/clusterProfiler.html) with the help of the 'ggplot2' package (version 3.5.1; https://cran.r-project.org/web/packages/ggplot2/index.html). The results were visualized with the 'ggplot2' R package and the results with P<0.05 were included in the present study.

Biomarker screening and performance evaluation. In the present study, three machine learning algorithms were used to screen out the characteristic genes of T2DM, including Least absolute shrinkage and selection operator (Lasso) logistic regression, Random forest (RF) and Support vector machine (SVM). The Lasso logistic regression analysis, RF algorithm and SVM algorithm were performed using the R packages 'glmnet,' (version 4.1-8; https://cran.r-project.org/web/packages/glmnet/index.html) 'randomForest' (version 4.7-1.2; https://cran.r-project.org/web/packages/randomForest/) and 'e1071' (version 1.7-16; https://cran.r-project.org/web/packages/e1071/index.html), respectively. Then, a Venn diagram obtained the intersection of the genes identified by the three algorithms and these genes are potential biomarkers.

After screening potential biomarkers, the expression differences of marker genes between normal and T2DM groups were further explored based on the GSE184050 dataset. The effect of each biomarker on the risk of T2DM was assessed by constructing line plots with the 'rms' package (version 7.0-0; https://cran.r-project.org/web/packages/rms/index.html) and the accuracy of the line plots was evaluated using calibration curves. At the same time, the R package 'pROC' (version 1.18.5; https://cran.r-project.org/web/packages/pROC/index.html) was used to plot the Receiver operating characteristic (ROC) curve and to calculate the area under the curve (AUC) to assess the predictive efficacy of the biomarkers independently as well as the overall predictive efficacy of the biomarkers. The overall predictive efficacy of the biomarkers was evaluated.

Analysis of immune cell infiltration. The present study explored the biological functions and related pathways of each biomarker by gene set enrichment analysis (GSEA; http://www.broadinstitute.org/gsea). To determine the relationship between infiltrating immune cells and candidate biomarkers in T2DM, the EPIC algorithm (http://epic.gfellerlab.org) was applied to assess the abundance of immune cells in T2DM samples from the GSE184050 dataset. The EPIC algorithm can accurately quantify the proportions of the different types of immune cells in the samples and analyze their changes between the disease state and the normal state. Based on the immune infiltration analysis results, the expression differences of immune checkpoint genes were compared between the normal and T2DM groups.

Subsequently, the relationships between biomarkers, immune infiltrating cells and immune checkpoints were explored using Pearson's correlation analysis in R and the 'ggplot2' R package visualized the results. P<0.05 indicates that the relationships were statistically significant.

Mendelian randomization (MR) analysis. Immune cells were used as exposure factors and significant instrumental variables for exposure factors (SNP) for exposure factors were selected from the Genome-wide association study (GWAS; https://gwas.mrcieu.ac.uk/) database as instrumental variables. To avoid the influence of strong linkage disequilibrium (LD) on the results, the thresholds of LD were set at r2 <0.3 and p1 <5e-8 (19). T2DM was used as the observed outcome and the outcome GWAS data GCST010118 was obtained from the GWAS database, including 77,418 East Asian cases and 356,122 East Asian controls. The 'TwoSampleMR' program package (version 2.0.1; https://cran.r-project.org/web/packages/twosamples/index.html) in R4.2.2 was used to perform the two-sample MR program method. SNP and outcome GWAS data were first preprocessed using the harmonise_data function in the TwoSampleMR program package to maintain a uniform format. MR Egger, Weighted median, Inverse variance weighted, Simple mode and Weighted mode methods were used for analysis. A heterogeneity test was also performed using the MR Egger method and inverse variance weighted (IVW) method to evaluate the heterogeneity of instrumental variables according to Cochrane's Q value. MR Egger regression equation was used to assess the horizontal polytropy of instrumental variables. In addition, to ensure that the results were not notably affected by a particular SNP, each SNP was removed in turn using the leave-one-out method. The present study compared the results of the IVW method with all variants (20). Three core assumptions ensured the accuracy of the causal estimation: i) The genetic instrumental variables are strongly associated with immune cells, ii) the genetic instrumental variables are independent of potential confounders iii) the genetic instrumental variables must influence the occurrence of T2DM only through immune cells.

Drug sensitivity analysis and molecular docking. The present study searched each of the key genes on the CTDbase database (https://ctdbase.org/) to obtain information about drug interactions and diseases associated with these genes. Subsequently, the small molecule ligands acting on the biomarker genes in T2DM were analyzed. The intersecting drugs of all the

marker genes via Venn diagrams were selected for subsequent molecular docking analysis.

Regarding molecular docking, first, the 2D structure of each small molecule ligand drug was obtained from the PubChem database (PDB, https://www.rcsb.org/). These structures were imported into Chem3D software to calculate the minimum free energy and convert them into three-dimensional structures. The 3D structures of the target proteins (receptors) were then obtained from the RCSB protein database (https://www.rcsb.org/). The structures were imported into PyMOL (https://www.pymol.org/) to remove water molecules and ligands. Receptors and ligands were prepared using AutoDock 1.5.6 (The Scripps Research Institute; https://autodock.scripps.edu/download-autodock4/) to obtain their PDBQT format and 3D mesh boxes were created for the receptors for subsequent molecular docking simulations. Next, molecular docking analysis was performed using AutoDock Vina 1.1.2 (The Scripps Research Institute; https://vina.scripps.edu/downloads/) to assess the binding energy between the ligand and receptor. Finally, the best predicted binding sites were visualized using PyMOL. Binding energies less than-5 kcal/mol were defined as indicating effective ligand-receptor binding and binding energies less than -7 kcal/mol indicated strong binding activity (21).

Single-cell sequencing analysis. First, single-cell data were read using the Read10X_h5 function in the 'Seurat' package for data preprocessing, which helps to remove potentially low-quality cells and dead cells to ensure the reliability of the analysis results. Subsequently, the batch effect was removed using the Integration method provided by the FindIntegrationAnchors function in the 'Seurat' package. The effect of batch effect removal was checked by t-Distributed Stochastic Neighbor Embedding (tSNE) dimensionality reduction analysis to ensure the accuracy and consistency of the data. Next, cell clustering analysis was performed using the 'Seurat' package. The graph was then partitioned into highly interconnected 'clusters' using a graph partitioning algorithm. The FindClusters function was used to perform the graph-based clustering analysis and the resolution parameter set to 0.3 to obtain different cell clusters. The cell clusters were also screened for differential genes using the FindMarkers function, in which the logfc was entered. Threshold parameter was set to 1 and the Wilcoxon test (test. use='Wilcox') used to identify the characteristic genes of each cell cluster. In this way, it was possible to pinpoint genes that were differentially expressed in different cell clusters. To further annotate cell subclusters, the 'SingleR' package continued to be used for cell subcluster annotation. By integrating known cell type marker genes, each cell cluster was annotated to a specific cell type or subpopulation. Next, the R package 'Cellchat' (version 2.1.0; https://github.com/jinworks/CellChat) was used to infer the number and strength of interactions between different cell clusters in the samples, revealing the interaction network between cell clusters, which provides important information for understanding cell function and tissue microenvironment.

Cell culture. RAW264.7 cells were cultured in Dulbecco's Modified Eagle's Medium (DMEM) containing 10% fetal bovine serum and 1% double antibiotic (penicillin 100 U/ml + streptomycin 100 μg/ml) and placed in an incubator at 37˚C containing 5% CO_2. The cell culture medium was changed every 2-3 days and when the cell density was 80-90%, the cells were routinely passaged.

Macrophage treatment. RAW264.7 cells were divided into the control group (Control), the high glucose (HG) group and the negative control (NG) group. The cells in the control group were cultured normally (containing 4.5 mmol/l glucose) without any treatment. The cells in the HG group were cultured in a DMEM medium containing HG (25 mmol/l) for 72 h. The cells in the NG group were cultured in a DMEM medium containing low glucose (5.5 mmol/l) for 72 h.

Macrophage polarization induction. To investigate the effect of T2DM on macrophage polarization, RAW264.7 cells were treated with TNF-α to induce M1 macrophage polarization and with IL-4 to induce M2 macrophage polarization. Control group cells were not treated in any way and were cultured normally. TNF-α-treated group cells (TNF-α group) were treated with TNF-α (20 ng/ml) for 24 h. IL-4-treated group cells (IL-4 group) were treated with IL-4 (20 ng/ml) for 24 h.

Cell grouping and transfection. The sequences of the small interfering RNA specifically targeting OAS3 (siRNA#1-OAS3), siRNA#2-OAS3, siRNA#1-MAP1B, siRNA#2-MAP1B and their negative control (siNC) are shown in Table I. RAW264.7 cells were divided into siNC group, siRNA#1-OAS3 group, siRNA#2-OAS3 group, siRNA#1-MAP1B group, siRNA#2-MAP1B group, HG + siRNA-OAS3 group and TNF-α + siRNA-OAS3 group. The siNC group cells were transfected with siNC. siRNA#1-OAS3 group, siRNA#2-OAS3 group, siRNA#1-MAP1B group and siRNA#2-MAP1B group cells were transfected with the corresponding siRNA, respectively. The cells in the HG + siRNA-OAS3 group were treated with HG and transfected with siRNA#1-OAS3. The cells in the TNF-α + siRNA-OAS3 group were treated with TNF-α and transfected with siRNA#1-OAS3.

For cell transfection, the siRNA was first dissolved into a master mix at a concentration of 20 μM and then RNATransMate (Beyotime Institute of Biotechnology) and siRNA were mixed in a serum-free medium and incubated at 25˚C for 20 min to form a siRNA/RNATransMate complex. Subsequently, 400 μl siRNA/RNATransMate complex and 1,600 μl serum-free medium were mixed, added to the culture plate, and incubated with the cells ($2x10^5$ cells/well) at 37˚C in a 5% CO_2 atmosphere for 24 h. A total of 48 h post-transfection, the medium was replaced with fresh complete medium to ensure cell viability.

RNA extraction and reverse transcription-quantitative (RT-q) PCR. Prior to RT-qPCR analysis, total RNA was extracted from the treated cells ($1x10^6$ cells/well) by RNeasy Plus Mini kit (cat. no. 74134; Qiagen GmbH) according to the instructions in the product manual. Then, the cDNA was synthesized with a QuantiTect Reverse Transcription kit (cat. no. 205311; Qiagen GmbH) according to the manufacturer's protocol. Finally, the RT-qPCR reactions mix solution (including Hieff UNICON Universal Blue Qpcr SYBR, Green Master Mix, PCR Forward Primer, PCR Reverse Primer, template DNA, ddH_2O) was prepared using the Hieff UNICON Universal

Table I. siRNA sequences.

Gene name	5'-3'	5'-3'
Negative control	UUCUCCGAACGUGUCACGUTT	ACGUGACACGUUCGGAGAATT
mMap1b-5496	GCUAUUUGAUACAAUGCAATT	UUGCAUUGUAUCAAAUAGCTT
mMap1b-2330	GGAAAGUCAAAGUCAUUAATT	UUAAUGACUUUGACUUUCCTT
mOas3-1493	GGGAGAAGAGUGUAUACAATT	UUGUAUACACUCUUCUCCCTT
mOas3-2418	GGACAAAUUCAUCAGUGAATT	UUCACUGAUGAAUUUGUCCTT

siRNA, small interfering RNA.

Table II. Primers for reverse transcription-quantitative PCR.

Gene name	Sequence
MAP1B-Forward	GTCTCCTTTACGCAGTCCTCC
MAP1B-Reverse	TGCTTTCCATTCTTCCCTTCA
OAS3-Forward	TGGGTGCCATGCGAATGTTGC
OAS3-Reverse	CTCCAGAGCGGGGCTGTCCTA
CD68-Forward	ACCGTGACCAGTCCCTCTT
CD68-Reverse	TGTCGTCTGCGGGTGATGC
CD80-Forward	CTTTGTGCTGCTGATTCGT
CD80-Reverse	TTTGCCAGTAGATTCGGTC
CD86-Forward	ATGGGCTCGTATGATTGT
CD86-Reverse	TCTTAGGTTTCGGGTGAC
CD32-Forward	GCAAAGGAAGTCTAGGAAGGA
CD32-Reverse	ATAATAACAATGGCTGCGACA
CD206-Forward	CATCACCAACGACCTCAG
CD206-Reverse	AGTAAGCCCTCTGTCTCC
CD204-Forward	ACTTGATACTGACAGGAAACC
CD204-Reverse	ATGTATAAAATTGTGAGCCAC
CD163-Forward	CCAGTCCAAACAACAAGC
CD163-Reverse	CACATTGGCATCAGTCATA
TNF-α-Forward	GCGGTGCCTATGTCTCAG
TNF-α-Reverse	TCCTCCACTTGGTGGTTT
GAPDH-Forward	GGGTCCCAGCTTAGGTTCAT
GAPDH-Reverse	CCAATACGGCCAAATCCGTT

Blue qPCR SYBR Green Master Mix (cat. no. 11184ES08; Shanghai Yeasen Biotechnology Co., Ltd.) following the manufacturer's instructions. Next, qPCR was performed using the LightCycler 480 II system (Roche Diagnostics). The qPCR cycling conditions were as follows: Initial denaturation at 95˚C for 30 sec, followed by 40 cycles at 95˚C for 5 sec and 60˚C for 30 sec. All experiments were independently replicated three times. The results were analyzed and quantified using the $2^{-\Delta\Delta Cq}$ method (22), GAPDH was used as an endogenous control and sequences of all primers were listed in Table II.

Western blotting. First, PMSF (cat. no. HKW2017; Jiangsu Haoke Bioengineering Co., Ltd.) and phosphorylated protease inhibitor (cat. no. HKW2018; Jiangsu Haoke Bioengineering Co., Ltd.) were mixed into IP lysis buffer (cat. no. HKW2012; Jiangsu Haoke Bioengineering Co., Ltd.) to extract the total protein from the cells. Then, the BCA working solution was prepared using the BCA Protein Quantification Kit (cat. no. HKW2019; Jiangsu Haoke Bioengineering Co., Ltd.). After the concentration of protein samples was detected using the Enhanced BCA Protein Assay Kit (cat. no. P0009; Beyotime Institute of Biotechnology), 30 μg protein/lane was subjected to SDS-PAGE on 10% gels. Subsequently, the separated proteins were transferred to a PVDF membrane (cat. no. 36125ES03; Shanghai Yeasen Biotechnology Co., Ltd.), after which the PVDF membrane was blocked with 5% skimmed milk (cat. no. SW3015, Nestle) at 25˚C for 1 h. Next, the PVDF membrane was incubated with diluted primary antibodies at 4˚C overnight and incubated with secondary antibodies at room temperature (25˚C) for 1 h. Then, the PVDF membrane was washed and treated with an ECL Plus working solution (cat. no. HKW2095; Jiangsu Haoke Bioengineering Co., Ltd.). The results were analyzed with the help of a Chemiluminescence system (Clinx Science Instruments Co., Ltd.) and were semi-quantified with ImageJ software (version 1.53m; National Institutes of Health). All information on antibodies is listed in Table III.

Statistical analysis. All bioinformatics-related statistical analyses in the present study were performed using R software 4.2.2 (https://www.r-project.org/) (23). The Pearson correlation test was used to determine the significance of correlations between variables and the Wilcoxon test was used to assess the importance of differences between the two groups. All cellular experimental data displays are the mean ± standard deviation of three biological replicates. GraphPad Prism 10.1.3 (Dotmatics) was used for statistical analysis, data processing and presentation of all experiments in the present study. One-way ANOVA and Tukey's post hoc test were used for multi-group comparisons. $P<0.05$ was considered to indicate a statistically significant difference.

Results

Screening of DEGs in T2DM and co-expression module construction. To screen for DEGs in T2DM, the present study first analyzed the GSE184050 database and identified 791 DEGs in T2DM, including 769 upregulated genes and 22 downregulated genes (Fig. 1). To further explore the key genes associated with T2DM, gene co-expression modules were established using WGCNA and 23 co-expression modules

Table III. All antibodies information in western blotting in the present study.

Name	Catalog number	Company	Molecular weight	Dilution
OAS3	21915-1-AP	Proteintech Group, Inc.	100-121 kDa	1:1,000
CD86	ET1606-50	Huabio	70 kDa	1:500
CD204	ER1913-21	Huabio	50 kDa	1:1,000
Phospho-mTOR (S2448)	HA600094	Huabio	289 kDa	1:1,000
GAPDH	10494-1-AP	Proteintech Group, Inc.	36 kDa	1:5,000
HRP Anti-Rabbit IgG (H+L)	SA00001-2	Proteintech Group, Inc.		1:5,000
HRP Anti-Mouse IgG (H+L)	SA00001-1	Proteintech Group, Inc.		1:5,000

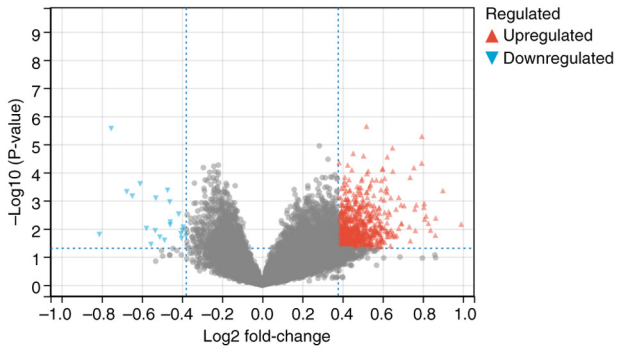

Figure 1. Identification of DEGs between T2DM and normal samples. The blue dots represent downregulated genes and the red dots represent upregulated genes. DEGs, differentially expressed genes; T2DM, type 2 diabetes mellitus.

were identified, most of which showed positive correlations with each other, suggesting that they had some consistency in expression patterns (Fig. 2A-C). By setting a significance threshold of P<0.05, the present study screened out four gene co-expression modules that were highly correlated with T2DM, including 'darkermagenta', 'floralwhite', 'orangered4' and 'dark grey'. Subsequently, in order to further screen mitochondrial dysfunction-related genes, 9,189 mitochondrial dysfunction-related genes were obtained from the GeneCard database. The mitochondrial dysfunction-related genes were intersected with the DEGs obtained from the GSE184050 database and T2DM-related genes obtained from the WGCNA and then a total of 65 genes were obtained (Fig. 2D). The specific names of the genes are shown in Table IV.

Functional enrichment analysis of mitochondrial dysfunction-related genes in T2DM. Then, to preliminary elucidate the underlying regulatory mechanisms of mitochondrial dysfunction in T2DM, the obtained 65 genes were subjected to functional enrichment analysis. The results of GO enrichment analysis showed that the aforementioned 65 genes were involved in biological processes (BP) such as substance transport, response to stress and chemicals, regulation of biological quality and immune system processes (Fig. 3A); and these genes were mainly enriched in the regions of the endomembrane system, cytosol, vesicles, extracellular space and organelle membrane (Fig. 3B); furthermore, these genes were mainly associated with enzyme binding, oxidoreductase activity, active transmembrane transporter activity, receptor ligand activity and antigen binding-related molecular processes (Fig. 3C). KEGG enrichment analysis showed that the aforementioned 65 genes were mainly involved in biological pathways such as necroptosis, NOD-like receptor signaling pathway, Th17 cell differentiation, ferroptosis, D-glutamine and D-glutamate metabolism (Fig. 3D). The aforementioned findings suggest that mitochondrial dysfunction-related genes in T2DM affect disease progression through multiple pathways.

Screening of biomarkers and validation of their predictive efficacy. Next, to screen T2DM biomarkers, the present study analyzed the key genes with a strong correlation with T2DM from the 65 genes mentioned aforementioned using three commonly used machine learning algorithms, namely Random forest (RF), SVM and Lasso logistic regression, respectively (Fig. 4A-C). Then, five key genes associated with T2DM were identified by plotting Venn diagrams, which were ERAP2, HLA-DQB1, HLA-DRB5, MAP1B and OAS3 (Fig. 4D). By analyzing the GSE184050 dataset, we found that ERAP2 was notably downregulated while HLA-DQB1, HLA-DRB5, MAP1B and OAS3 were upregulated in T2DM (Fig. 5A-E; P<0.05).

In addition, the performance of ERAP2, HLA-DQB1, HLA-DRB5, MAP1B and OAS3 in the prediction of T2DM were further analyzed. MAP1B showed the best performance (AUC=0.759), while HLA-DRB5 had the worst predictive efficacy (AUC=0.574) in the prediction of T2DM (Fig. 5F). In addition, the results of the nomogram showed that the higher the expression levels of HLA-DQB1, HLA-DRB5, MAP1B and OAS3 and the lower the expression level of ERAP2, the higher the probability of T2DM occurrence (Fig. 6A). In addition, the calibration curves were almost identical to the ideal curves, indicating that our prediction model had high accuracy (Fig. 6B). And the overall predictive efficacy AUC value of the five marker genes reached 0.833, which was notably higher than the predictive efficacy of individual genes (Fig. 6C).

Target compound prediction and molecular docking. The present study identified target compounds for each of the five markers: 42 for ERAP2, 106 for OAS3, 59 for HLA-DQB1, 28 for HLA-DRB5 and 170 for MAP1B. The Venn diagram revealed two common compounds, valproic acid (VPA) and aflatoxin B1 (AFB1; Fig. 7A). Since VPA is used in cancer treatment and AFB1 is a carcinogen, only VPA was chosen for molecular

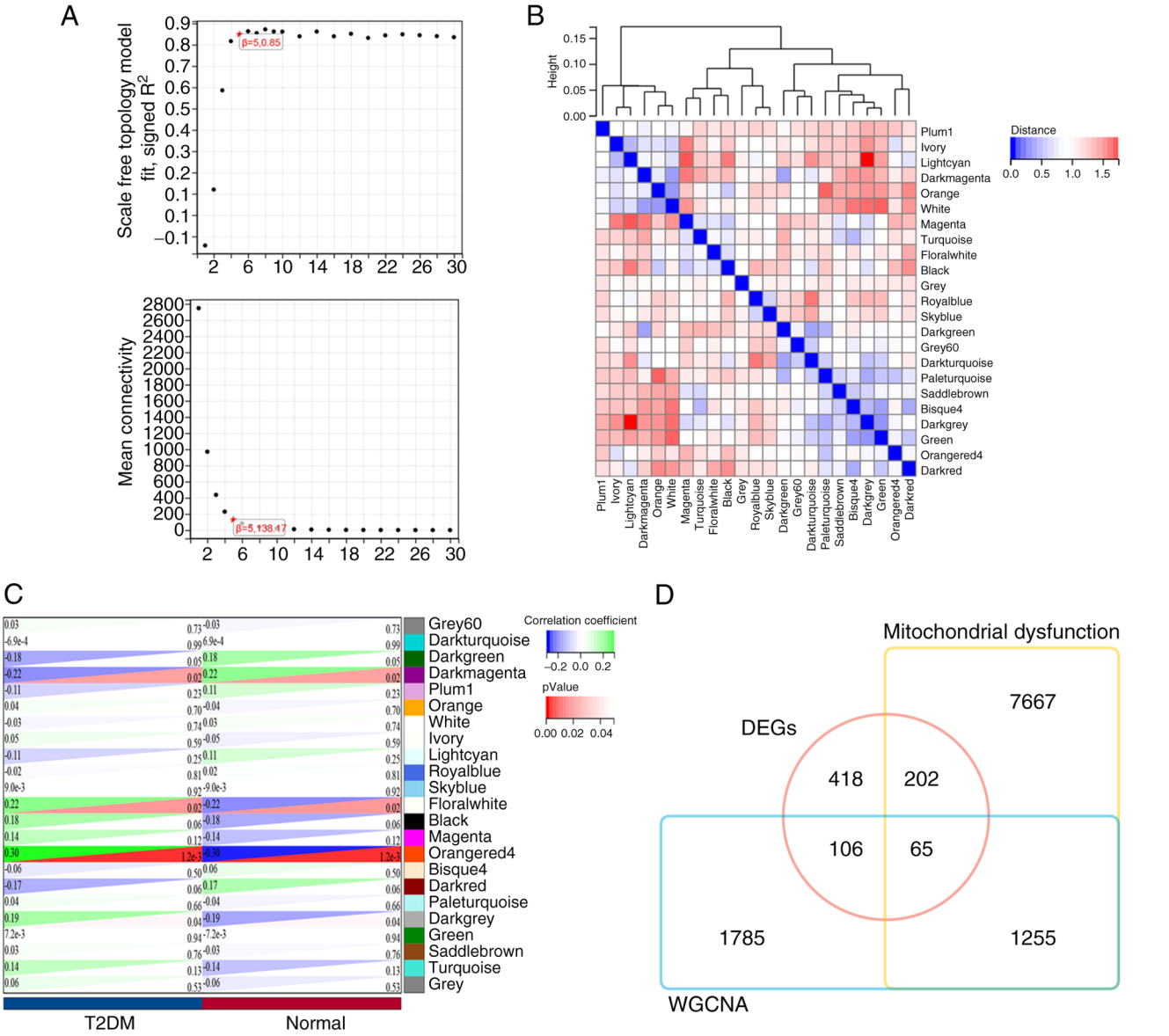

Figure 2. Screening for mitochondrial dysfunction and intersection of T2DM-related genes. (A) Determination of appropriate soft thresholds based on scale independence and average connectivity. (B) Results of Pearson correlation analysis of 23 co-expression modules. (C) Results of correlation analysis between modules and traits in T2DM (blue: negative correlation, green: positive correlation). (D) Screening for mitochondrial dysfunction and intersection of T2DM-related genes. T2DM, type 2 diabetes mellitus.

docking with the five markers in the next study. Molecular docking results revealed that VPA formed stable hydrogen bonds with several proteins: ERAP2 (ARG185, LYS848, GLU813, TYR812), HLA-DQB1 (SER139, ARG149, LEU147), HLA-DRB5 (GLY1, GLY14), MAP1B (GLY1, GLY14, SER288, LYS375) and OAS3 (GLY66, ASN193) (Fig. 7B-F).

Correlation analysis of biomarkers and immune microenvironment. T2DM is a metaflammatory disease. MR analysis explored the link between $CD4^+$ and $CD8^+$ T cells and T2DM. The IVW test revealed a negative correlation between T2DM risk and GCST90001482 (Resting CD4 regulatory T cell), GCST90001492 (Secreting CD4 regulatory T cell) and GCST90001499 (Activated and resting CD4 regulatory T cell), while GCST90001548 (Central Memory CD8+ T cell) showed a positive correlation. The MR analysis (Table V) revealed significant associations between mitochondrial dysfunction-related genetic variants and T2DM risk mainly using the IVW method. Specifically, exposure factors GCST90001482, GCST90001548, GCST90001492 and GCST90001499 demonstrated causal effects on T2DM susceptibility ($P<0.05$). Additionally, heterogeneity tests (Table VI) indicated no substantial variability across genetic instruments (IVW Q-test P-values: 0.052-0.806), supporting homogeneity of effect estimates. Horizontal pleiotropy tests (Table VII) further confirmed the absence of significant bias (MR Egger intercept P-values: 0.250-0.843), validating the robustness of causal inferences. Collectively, these findings underscore mitochondrial dysfunction-related genes as potential contributors to T2DM progression, with minimal confounding from heterogeneity or pleiotropy ($P>0.05$). The error line remained stable after removing each SNP (Fig. S1), confirming the reliability and robustness of the predictions.

Table IV. Mitochondrial dysfunction-related genes in type 2 diabetes mellitus.

Gene name	Full name	Gene name	Full name
MAP1B	Microtubule-associated protein 1B	RIN3	Ras and Rab interactor 3
RAB7A	Rab protein member 7A	SPI1	Spi-1 proto-oncogene
RHOG	Ras homolog family member G	IRGM	Immunity-related GTPase family M
HBA1	Hemoglobin subunit alpha 1	OAS3	2'-5'-Oligoadenylate synthetase 3
HBA2	Hemoglobin subunit alpha 2	CHERP	Calcium homeostasis endoplasmic reticulum protein
SLC24A4	Solute carrier family 24, member 4	HBG2	Hemoglobin subunit gamma 2
HBB	Hemoglobin subunit beta	INF2	Inverted formin, FH2 and WH2 domain containing
ERAP2	Endoplasmic reticulum aminopeptidase 2	ALOX15	Arachidonate 15-lipoxygenase
RNPEPL1	Arginyl aminopeptidase-like 1	CXCR3	C-X-C motif chemokine receptor 3
SLC26A1	Solute carrier family 26, member 1	ZBTB7A	Zinc finger and BTB domain containing 7A
MTHFS	5,10-methenyltetrahydrofolate synthetase	CXCL8	C-X-C motif chemokine ligand 8
TECR	Trans-2,3-enoyl-CoA reductase	HSPB1	Heat shock protein family B (small) member 1
CASZ1	Castor zinc finger 1	HLA-DQB1	Major histocompatibility complex, class II, DQ beta 1
GLUD2	Glutamate dehydrogenase 2	HBG1	Hemoglobin subunit gamma 1
SLC25A22	Solute carrier family 25, member 22	UTS2	Urotensin 2
ABCD1	ATP binding cassette subfamily D member 1	TUBB2A	Tubulin beta 2A class IIa
OXT	Oxytocin/neurophysin I prepropeptide	LTBP3	Latent transforming growth factor beta binding protein 3
TAPBP	TAP binding protein (tapasin)	UCP2	Uncoupling protein 2
SERPINA1	Serpin family A member 1	CBFA2T3	Core-binding factor, runt domain, alpha subunit 2; translocated to, 3 (homolog of mouse)
CSF1	Colony stimulating factor 1	ADORA3	Adenosine A3 receptor
PML	Promyelocytic leukemia	TICAM1	Toll-like receptor adaptor molecule 1
NPHP4	Nephrocystin 4	NRGN	Neurogranin
TEX22	Testis expressed 22	NLRP6	NLR family pyrin domain containing 6
HBD	Hemoglobin subunit delta	ZFPM1	Zinc finger protein, FOG family member 1
CD7		PANX2	Pannexin 2
SLC29A1	Solute carrier family 29, member 1	FTH1	Ferritin heavy chain 1
MIER2	Mesoderm induction early response 1, family member 2	DLGAP4	DLG associated protein 4
OLIG1	Oligodendrocyte transcription factor 1	TMTC1	Transmembrane and tetratricopeptide repeat containing 1
TGFB1	Transforming growth factor beta 1	SCAMP4	Secretory carrier membrane protein 4
ARID1A	AT-rich interaction domain 1A	HLA-DRB5	Major histocompatibility complex, class II, DR beta 5
ELANE	Elastase, neutrophil expressed	AHDC1	AT-hook DNA binding motif containing 1
JUND	JunD proto-oncogene, AP-1 transcription factor subunit	CBS	Cystathionine-beta-synthase
PABPN1	Poly(A) binding protein nuclear 1		

Subsequently, the present study analyzed the expression levels of the aforementioned five biomarkers in immune cells. The results of the GSEA analysis indicated that the five biomarkers screened may be associated with IL-2 and IL-6 pathways, suggesting that they are associated with immune infiltration in T2DM (Fig. S2). Therefore, a detailed analysis was performed of the immune infiltration of T2DM using the EPIC algorithm. It was found that the number of $CD4^+$ T cells

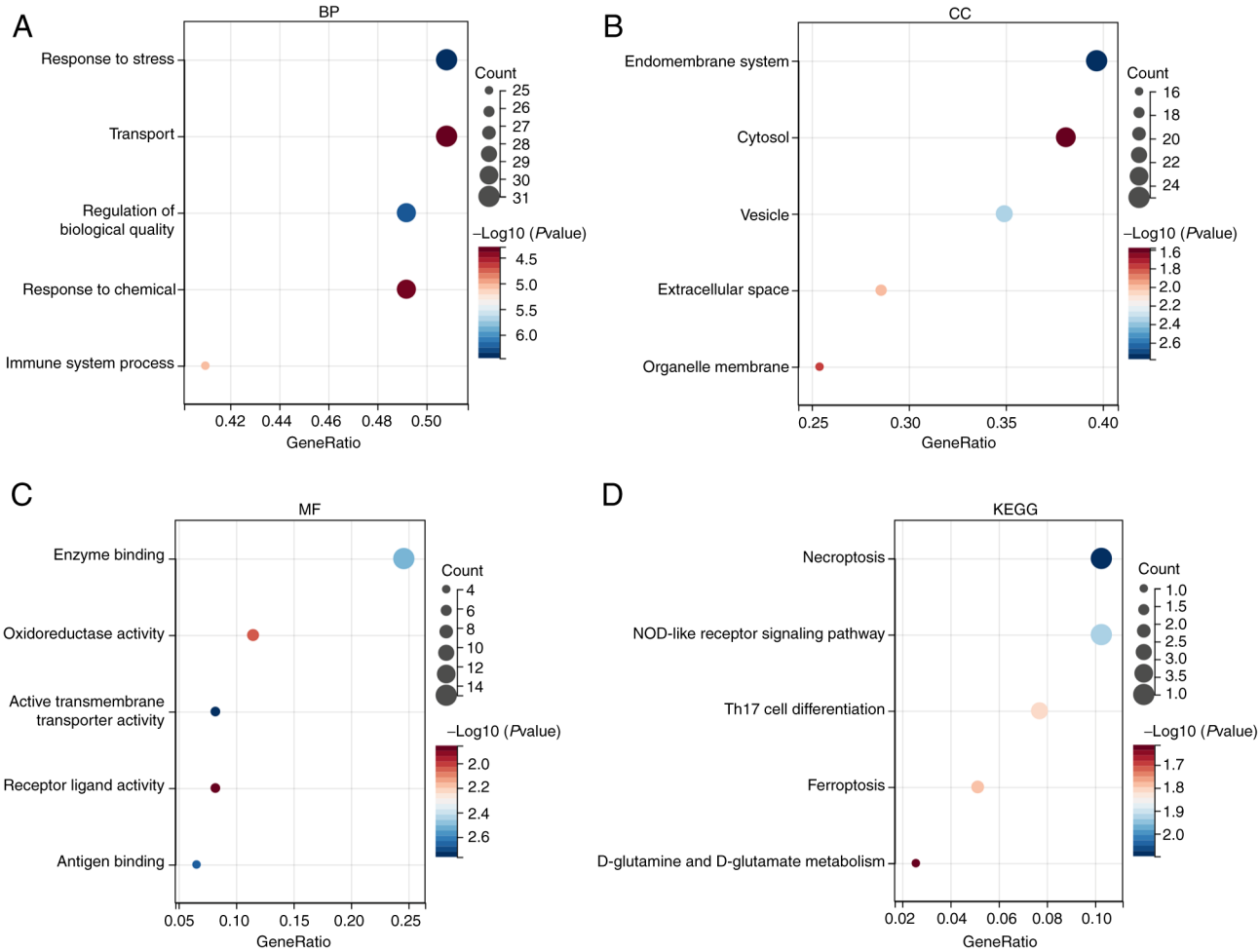

Figure 3. Functional enrichment analysis of 65 key genes. The results of GO analysis demonstrated the key genes before their critical roles in (A) MF, (B) CC and (C) BP. (D) Results of KEGG analysis demonstrated the key genes' important pathways. GO, Gene Ontology; MF, molecular function; CC, cellular component; BP, biological process; KEGG, Kyoto Encyclopedia of Genes and Genomes.

and $CD8^+$ T cells in T2DM was notably lower than that in the normal group; TNFRSF4, CEACAM1, PDCD1, SIRPA, ICOSLO, BTN2A2 and BTN2A1 were notably upregulated, while CD86, HLA-DMB, HLA-DOA and HLA-DPB1 was notably downregulated in the T2DM (Fig. 8A and B; $P<0.05$). Pearson correlation analysis showed that. OAS3 and MAP1B were negatively correlated with $CD8^+$ T cells, while ERAP2 was positively correlated with $CD8^+$ T cells (Fig. 8C; $P<0.05$). These suggested that changes in $CD8^+$ T cells may affect the expression of these marker genes, which in turn affects the immune microenvironment in diabetes. In addition, MAP1B was notably correlated with all immune checkpoint genes except PDCD1 (Fig. 8C; $P<0.05$). The aforementioned findings suggested that MAP1B may regulate the development of diabetes by modulating the immune checkpoint pathway.

Results of single-cell sequencing analysis. The formation of islet inflammatory microenvironment and the interaction between immune cells have gradually attracted attention. Therefore, T2DM single-cell transcriptional profiles based on the GSE221156 dataset were analyzed. As shown in Fig. 9A and B, 27 cell populations were obtained by tSNE clustering analysis and seven major cell subpopulations, including epithelial cells, neuronal cells, smooth muscle cells, tissue stem cells, endothelial cells, macrophages and T cells, were identified by cell type annotation with the 'SingleR' package. Analysis of the results of cell interactions showed that each cell type was associated with each other to varying degrees, with tissue stem cells being the most strongly related to other cells (Fig. S3) and macrophages and T cells being important in the immune response (Fig. 9C). Subsequently, the expressions of the five biomarkers in cells were further analyzed and it was found that MAP1B was expressed in almost all cell types, but particularly in neuronal cells and tissue stem cells; ERAP2 was more prominently expressed in endothelial cells and HLA-DQB1, HLA-DRB5 and OAS3 were more prominently expressed in macrophages (Fig. 9D). Notably, the expression of the five marker genes was more prevalent in macrophages, suggesting that the role of these marker genes in T2DM may be closely related to macrophage function. Therefore, subsequent experiments endeavored to investigate the roles of the aforementioned five biomarkers in T2DM via cellular experiments.

Detection of MAP1B and OAS3 expression levels in macrophages. In the aforementioned single-cell sequencing analysis results, five marker genes commonly expressed in macrophages were identified. The expression of these markers in T2DM-associated macrophages was then verified by cellular

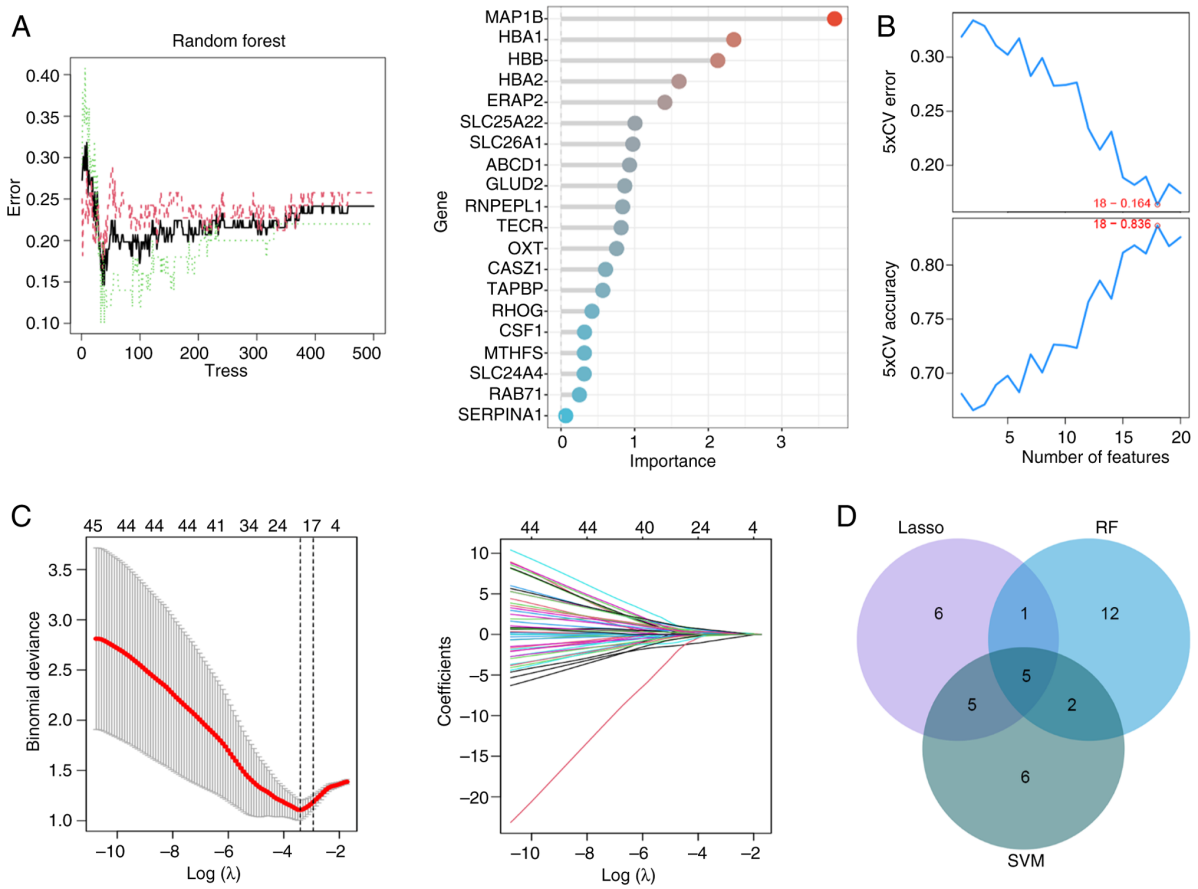

Figure 4. Screening of biomarkers. (A) RF was used to screen biomarkers and rank the genes according to importance. (B) SVM was used to screen biomarkers. (C) Lasso logistic regression algorithm was used to screen biomarkers with different colors denoting different genes. (D) Venn diagrams was used to screen common potential biomarkers obtained from all three algorithms. RF, Random forest; SVM, support vector machine; Lasso, least absolute shrinkage and selection operator.

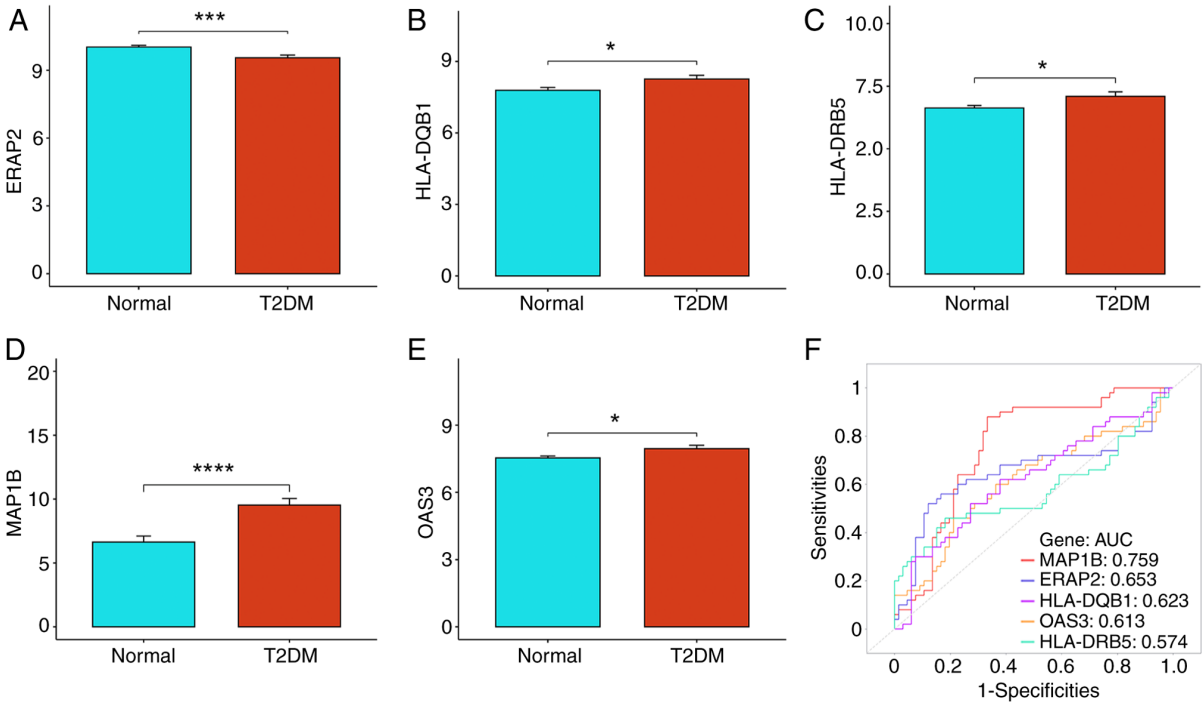

Figure 5. Expression and predictive efficacy analysis of biomarkers in T2DM. (A-E) Expression levels of five biomarkers in the normal and T2DM groups. (A) ERAP2, (B) HLA-DQB1, (C) HLA-DRB5, (D) MAP1B and (E) OAS3. (F) ROC curves of five biomarkers independently predicting efficacy in T2DM. *P<0.05, ***P<0.001 and ****P<0.0001. T2DM, type 2 diabetes mellitus; ERAP2, endoplasmic reticulum aminopeptidase 2; HLA, human leukocyte antigen; MAPIB, microtubule-associated protein 1B; OAS3, 2'-5'-oligoadenylate synthetases 3; ROC, receiver operating characteristic; AUC, area under the curve.

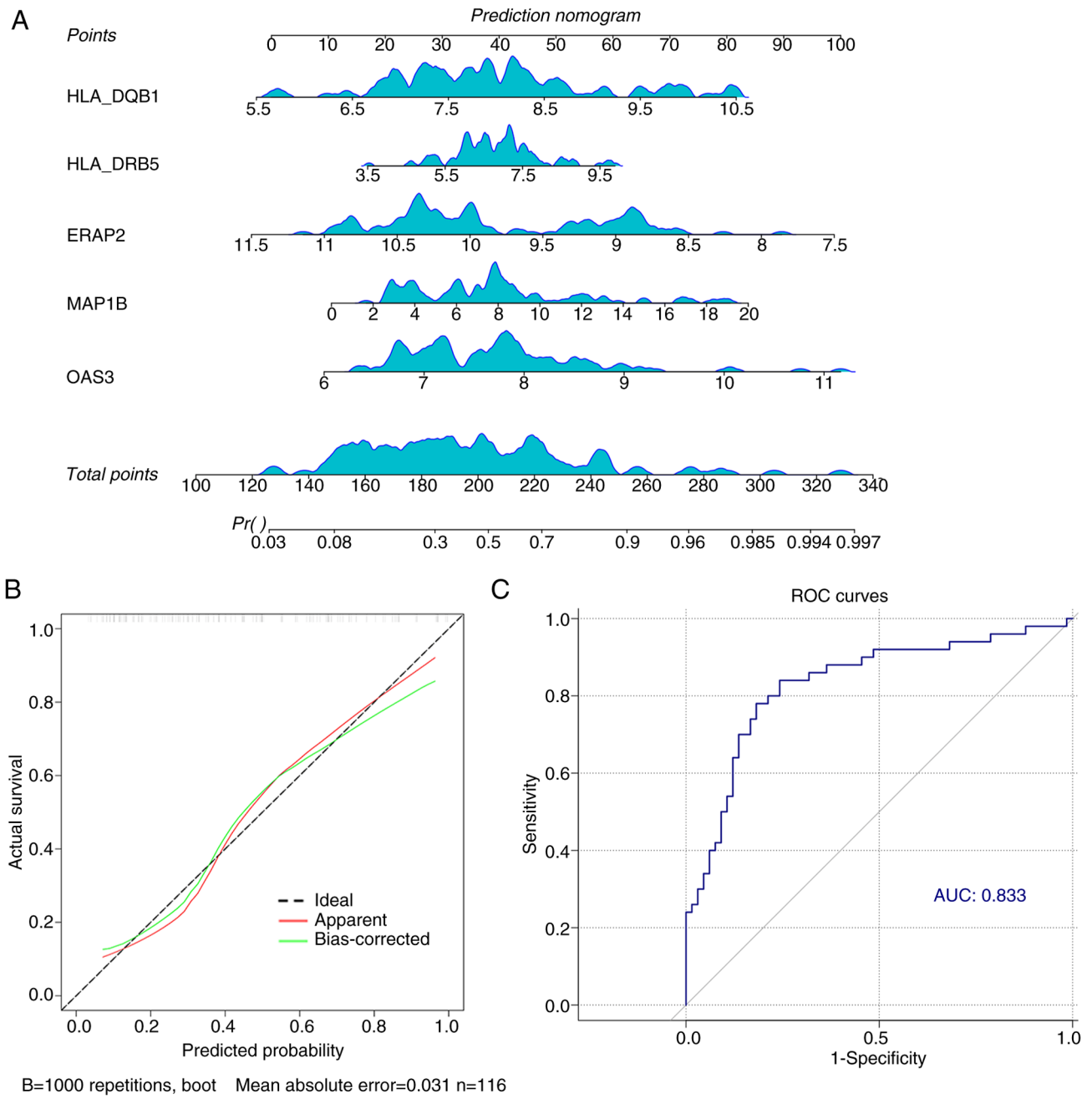

Figure 6. Analysis of the overall predictive efficacy of the five biomarkers. (A) A nomogram was constructed based on the five biomarkers. (B) The calibration curves were almost identical to the ideal curves. (C) ROC curve showing the overall prediction efficacy of the five marker genes. ROC, receiver operating characteristic; AUC, area under the curve; HLA, human leukocyte antigen; ERAP2, endoplasmic reticulum aminopeptidase 2; OAS3, 2'-5'-oligoadenylate synthetase 3.

experiments. Due to the absence of murine sequences for ERAP2, HLA-DQB1 and HLA-DRB5 in the NCBI database, only MAP1B and OAS3 were validated experimentally. The RT-qPCR results showed that the expressions of MAP1B and OAS3 were notably increased in the HG group (Fig. 10; $P<0.001$). The results indicated that HG concentration notably induced the expression levels of MAP1B and OAS3 in macrophages.

Analysis of M1/M2 macrophage polarization in T2DM. To further explore the effect of T2DM on macrophage polarization, the expression of M1 macrophage markers (CD68, CD80, CD86 and CD32) and M2 macrophage markers (CD206, CD204 and CD163) were examined (Fig. 11). The results showed that the expression of M1 macrophage markers (except for CD32) was notably increased and the expression of M2 macrophage markers were decreased considerably under HG conditions (Fig. 11; $P<0.01$). The aforementioned findings suggested that in an HG environment, M1 macrophages and pro-inflammatory responses increase, while M2 macrophages and anti-inflammatory responses decrease. Future studies on M1/M2 polarization will focus on CD86 and CD204, as they showed the most significant expression differences.

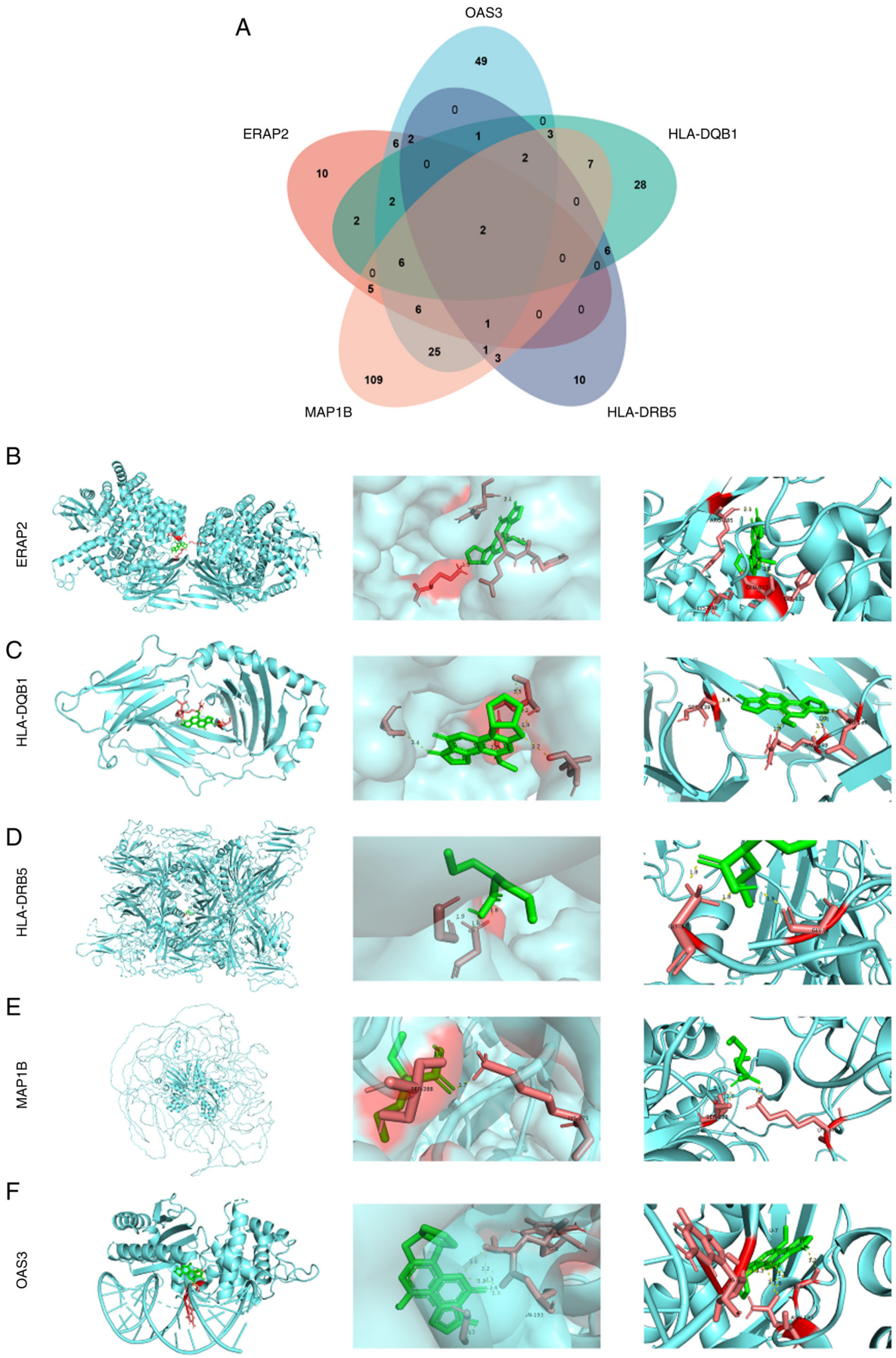

Figure 7. Biomarker targeting compounds and molecular docking results of five biomarkers VPA. (A) Biomarker targeting compounds. (B) Docking site of VPA with ERAP2. (C) Docking site of VPA with HLA-DQB1; (D) Docking site of VPA with HLA-DRB5; (E) Docking site of VPA with MAPIB; (F) Docking site of VPA with OAS3. VPA, valproic acid; ERAP2, endoplasmic reticulum aminopeptidase 2; HLA, human leukocyte antigen; MAPIB, microtubule-associated protein 1B; OAS3, 2'-5'-oligoadenylate synthetases 3; ROC, receiver operating characteristic; AUC, area under the curve.

Table V. Mendelian analysis between exposure factors and type 2 diabetes mellitus.

Exposure factor	Method	nSNP	b	SE	P-value	lo_ci	up_ci
GCST90001482	MR Egger	11	-0.070	0.095	0.478	-0.256	0.116
	Weighted median	11	-0.026	0.023	0.250	-0.071	0.019
	Inverse variance weighted	11	-0.051	0.023	0.027	-0.097	-0.006
	Simple mode	11	-0.020	0.052	0.710	-0.121	0.082
	Weighted mode	11	-0.025	0.025	0.335	-0.073	0.023
GCST90001492	MR Egger	8	-0.010	0.005	0.101	-0.020	0.000
	Weighted median	8	-0.008	0.005	0.071	-0.017	0.001
	Inverse variance weighted	8	-0.007	0.004	0.049	-0.015	0.000
	Simple mode	8	-0.007	0.012	0.574	-0.031	0.016
	Weighted mode	8	-0.008	0.004	0.096	-0.016	0.000
GCST90001499	MR Egger	14	-0.012	0.022	0.587	-0.055	0.030
	Weighted median	14	-0.011	0.014	0.429	-0.037	0.016
	Inverse variance weighted	14	-0.032	0.015	0.031	-0.060	-0.003
	Simple mode	14	-0.043	0.026	0.129	-0.094	0.009
	Weighted mode	14	-0.013	0.013	0.356	-0.038	0.013
GCST90001548	MR Egger	15	0.039	0.020	0.068	0.001	0.078
	Weighted median	15	0.023	0.016	0.159	-0.009	0.054
	Inverse variance weighted	15	0.025	0.012	0.032	0.002	0.048
	Simple mode	15	0.025	0.023	0.297	-0.020	0.070
	Weighted mode	15	0.025	0.014	0.101	-0.003	0.053

Table VI. Risk heterogeneity test for exposure factors and type 2 diabetes mellitus.

Exposure factor	Method	Q	Q_df	Q_pval
GCST90001482	MR Egger	24.956	9	0.302
	Inverse variance weighted	25.072	10	0.052
GCST90001492	MR Egger	3.233	6	0.779
	Inverse variance weighted	3.767	7	0.806
GCST90001499	MR Egger	25.259	12	0.136
	Inverse variance weighted	28.329	13	0.081
GCST90001548	MR Egger	13.850	13	0.384
	Inverse variance weighted	14.707	14	0.398

Table VII. Risk level horizontal pleiotropy test for exposure factors and type 2 diabetes mellitus.

Exposure factor	egger_ intercept	SE	P-value
GCST90001482	0.004	0.020	0.843
GCST90001492	0.003	0.004	0.493
GCST90001499	-0.007	0.006	0.250
GCST90001548	-0.005	0.005	0.386

Effects of MAP1B and OAS3 on macrophage M1/M2 polarization. To further investigate the effects of MAP1B and OAS3 in macrophage polarization, the present study initially assessed their expression levels in M1 and M2 macrophages. RAW264.7 cells were stimulated with TNF-α to induce M1 polarization and with IL-4 to induce M2 polarization. RT-qPCR analysis revealed a significant downregulation of MAP1B expression in the TNF-α group and a marked upregulation in the IL-4 group (Fig. 12A; $P<0.001$). Conversely, OAS3 expression was increased in the TNF-α group and decreased in the IL-4 group (Fig. 12B; $P<0.01$). These findings suggested that MAP1B is potentially associated with M2 macrophage polarization, whereas OAS3 appears to be linked to M1 macrophage polarization.

To assess the effects of MAP1B and OAS3 on macrophage polarization, siRNA was used to inhibit their expression. RT-qPCR showed siRNA#1-MAP1B was more effective than siRNA#2-MAP1B (Fig. 12C; $P<0.001$), while siRNA#2-OAS3 outperformed siRNA#1-OAS3 (Fig. 12F; $P<0.001$). Inhibiting

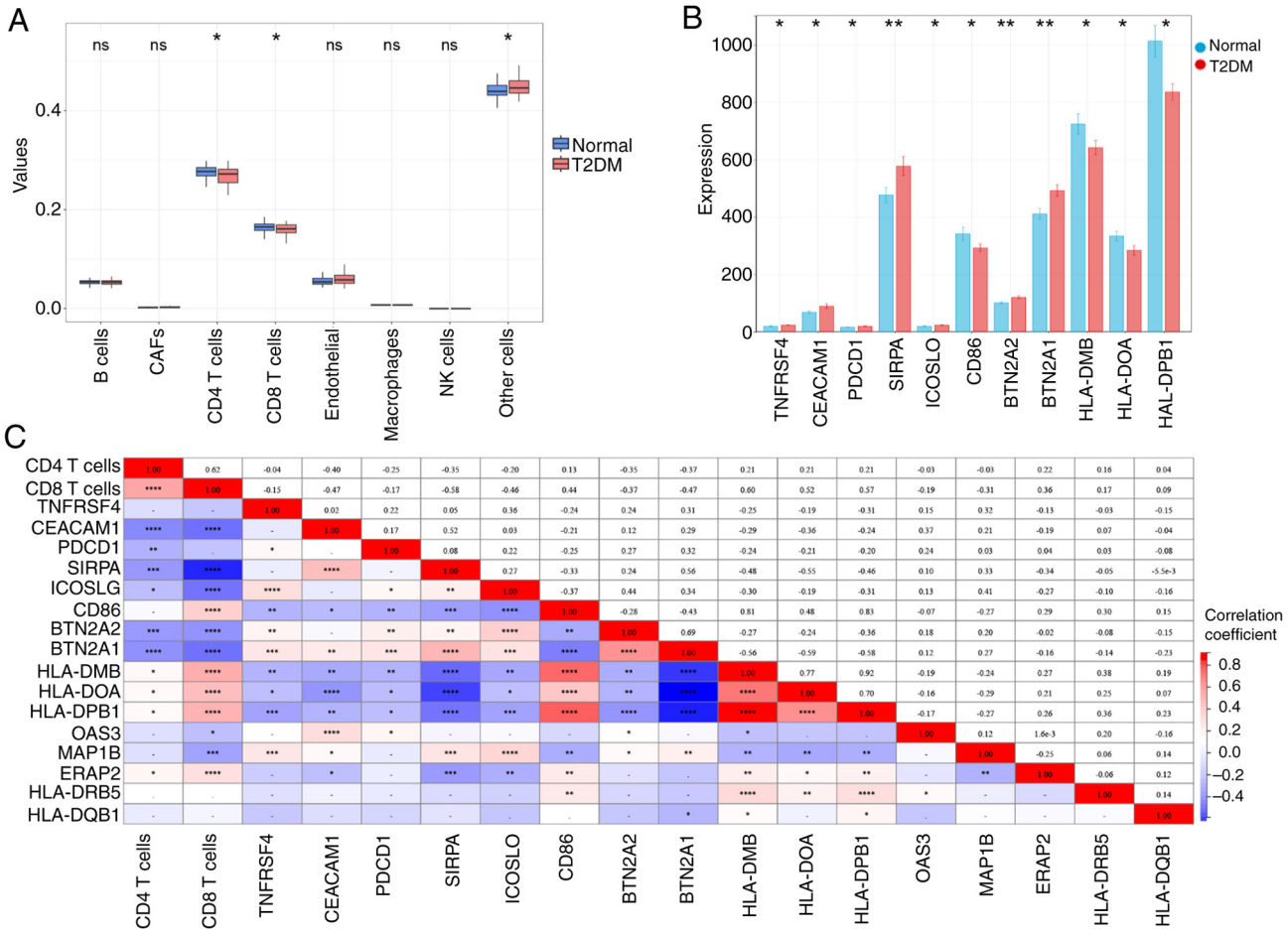

Figure 8. Correlation analysis of biomarkers with immune infiltration and immune checkpoint genes. (A) Analysis of immune infiltration; (B) Difference in expression of immune checkpoint genes in normal and T2DM groups; (C) Pearson correlation of immune cells, immune checkpoints and marker genes, with blue color indicating negative correlation and red color indicating positive correlation. *P<0.05, **P<0.01, ***P<0.001, ****P<0.0001.T2DM, type 2 diabetes mellitus; ns, no significant difference.

MAP1B increased M1 macrophage marker CD86 level and decreased M2 macrophage marker CD204 (Fig. 12D and E; P<0.001), whereas reducing OAS3 lowered CD86 and raised CD204 levels. (Fig. 12G and H; P<0.001). These results indicated that MAP1B promotes M2 macrophage polarization, whereas OAS3 promotes M1 macrophage polarization. Since significant M1 macrophage polarization in HG-induced RAW264.7 cells was observed in the aforementioned experiments, which is consistent with the role of OAS3, we aim to investigate the mechanism of OAS3 in macrophage polarization in depth in a follow-up study.

Downregulation of OAS3 expression attenuates M1 macrophage polarization by upregulating phosphorylated (p-) mTORC level. To explore the role of OAS3 expression on macrophage polarization in T2DM, the expression of OAS3 in HG-induced macrophages was knocked down by transfection with siRNA#2-OAS3. HG treatment notably increased the expression level of the M1 macrophage marker CD86 and notably decreased the expression level of the M2 macrophage marker CD204. By contrast, inhibition of OAS3 expression notably reversed the effect of HG treatment (Fig. 13A and B; P<0.001). The aforementioned data suggested that downregulation of OAS3 expression inhibited macrophage M1 polarization and promoted macrophage M2 polarization in a high-glucose environment, which attenuated the inflammatory response.

To further validate the role of OAS3 in M1 macrophage polarization, the OAS3 expression was downregulated in TNF-α-induced macrophages. The results of RT-qPCR and western blotting experiments showed that TNF-α treatment upregulated the expression of CD86 in macrophages and downregulation of OAS3 expression inhibited CD86 expression; moreover, downregulation of OAS3 reversed the TNF-α action (Fig. 13C and D; P<0.01). The results further indicated that OAS3 played a promoting role in M1 macrophage polarization and that downregulation of OAS3 notably inhibited M1-type polarization and attenuated inflammatory responses.

To explore the potential mechanism of OAS3-induced M1 macrophage polarization, GSEA was used and it was found that OAS3 showed activation in the mTORC1 signaling pathway (Fig. S2). Therefore, the effect of downregulation of OAS3 on proteins related to the mTORC1 signaling pathway in macrophages was examined. Western blotting results showed that there was no significant change in the levels of mTORC protein in each group (Fig. 13E). TNF-α induced a significant decrease in p-mTORC/mTORC protein levels in macrophages, whereas downregulation of OAS3 expression increased the

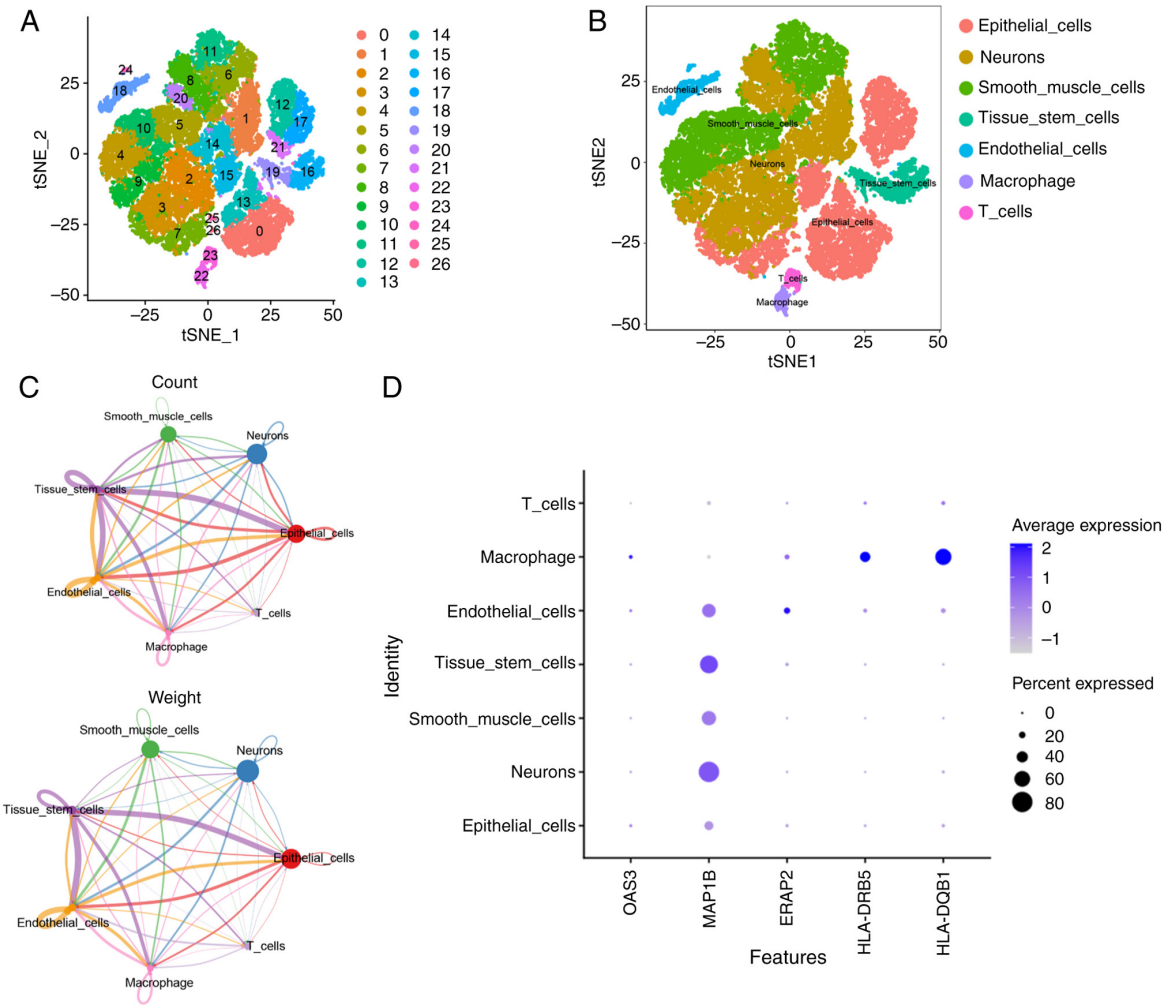

Figure 9. Analysis of cell types in T2DM based on single-cell sequencing data. (A) Cell populations identified by the GSE221156 dataset; (B) annotation of cell subpopulations. (C) Interaction diagram between cell types in 7. (D) Distribution of various cell types in normal, PD and T2DM samples. PD, prediabetic state; T2DM, type 2 diabetes mellitus; OAS3, 2'-5'-oligoadenylate synthetases; MAPIB, microtubule-associated protein 1B; ERAP2, endoplasmic reticulum aminopeptidase 2; HLA, human leukocyte antigen.

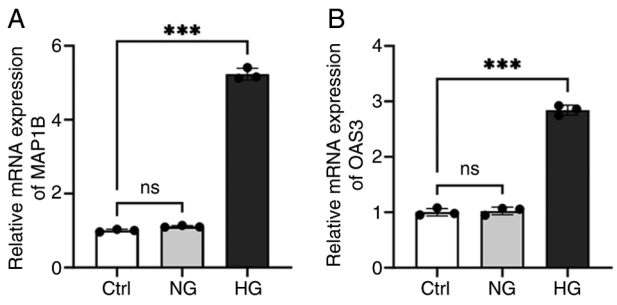

Figure 10. The expression levels of MAP1B and OAS3 were detected in RAW264.7 cells. (A) The expression of MAP1B was detected by RT-qPCR. (B) The expression of OAS3 was detected by RT-qPCR. ***P<0.001; ns, no significant difference. MAPIB, microtubule-associated protein 1B; OAS3, 2'-5'-oligoadenylate synthetases; RT-qPCR, reverse transcription-quantitative PCR; Ctrl, blank control group; NG, negative control group; HG, high glucose group.

value of p-mTORC/mTORC (Fig. 13E; P<0.001). In addition, downregulation of OAS3 expression reversed the effect of TNF-α, suggesting that downregulation of OAS3 expression attenuated macrophage M1 polarization by upregulating p-mTORC levels.

Discussion

Research has shown that there are a number of factors contributing to the global epidemic of diabetes, including an aging population, a sedentary lifestyle, obesity and an unhealthy daily diet (24). Prolonged hyperglycemia can cause damage to organs and tissues such as eyes, nerves, kidneys and cardiovascular organs, leading to a series of complications that pose a serious threat to human health and a huge burden on healthcare costs (12,25). The current classical drugs for the treatment of T2DM, such as metformin, sulfonylureas and thiazolidinediones, cause adverse reactions in patients to varying degrees (6). Therefore, through an in-depth study of the pathogenesis of T2DM and corresponding early analysis, the prediction, diagnosis and development of therapeutic drugs are of great significance to the clinical treatment of patients.

Currently, HbA1c is extensively utilized in the diagnosis of T2DM (8). Despite its high stability and convenience, it may result in misdiagnosis in certain cases, such as those involving

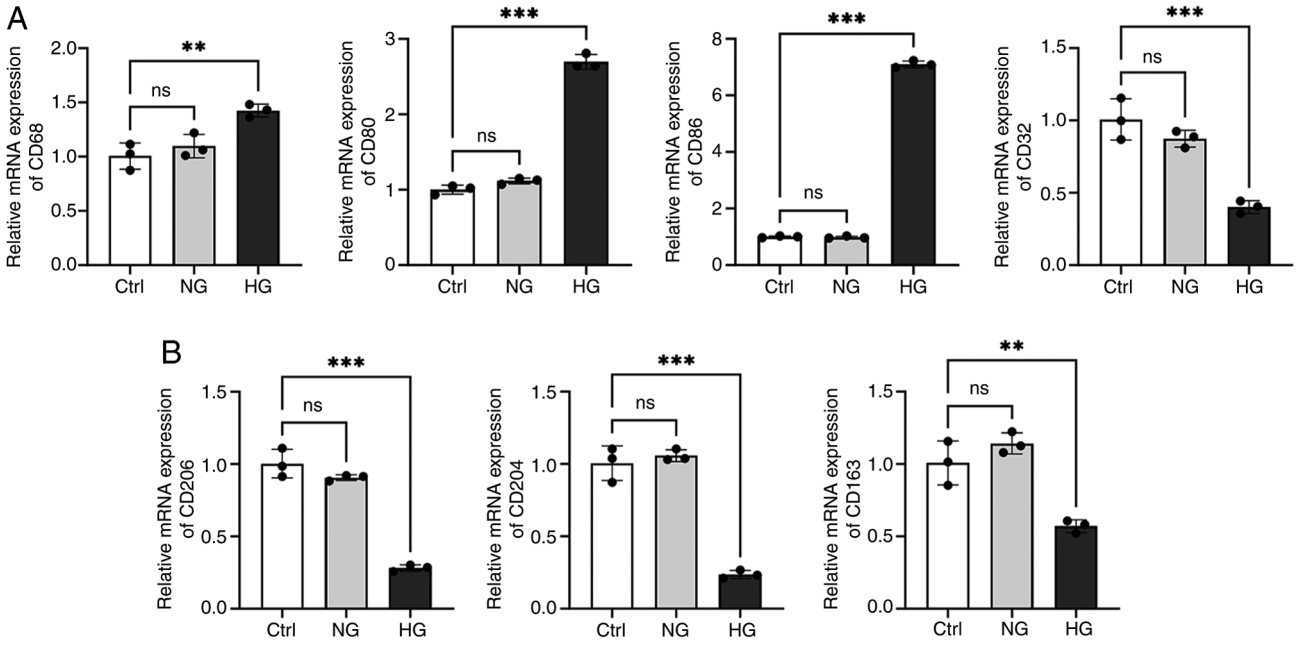

Figure 11. Detection of M1 macrophage and M2 macrophage polarization in T2DM. (A) Detection of the expression of M1 macrophage markers CD68, CD80, CD86 and CD32. (B) Detection of the expression of M2 macrophage markers CD206, CD204 and CD163. **P<0.01; ***P<0.001; ns, no significant difference; T2DM, type 2 diabetes mellitus; Ctrl, blank control group; NG, negative control group; HG, high glucose group.

anemia or ethnic differences (26). Fasting blood glucose (FPG) and the oral glucose tolerance test (OGTT) continue to be regarded as the gold standards for T2DM diagnosis, with OGTT being particularly sensitive in detecting early diabetes and prediabetes (27). Nevertheless, the complexity and cost associated with OGTT constrain its use in some regions. Consequently, novel biomarkers and assays for T2DM are being developed, which have the potential to transform future screening and diagnostic strategies for diabetes. Fructosamine and glycated albumin have been identified as valuable indicators for evaluating short-term glycemic control, particularly in patients necessitating frequent monitoring (28). A previous study proposed that fructosamine and glycated albumin may offer greater predictive value than HbA1c in certain populations (28). Furthermore, 1,5-AG serves as an additional marker for assessing short-term blood glucose fluctuations (29). 1,5-AG is particularly effective in monitoring postprandial hyperglycemia and its integration with HbA1c and FPG enhances the early detection rate of T2DM (29). These advances not only facilitate the early detection of diabetes but also enhance patient management and prognosis, thereby mitigating the risk of complications.

The pathogenesis of T2DM is characterized by a gradual loss of insulin secretion from β-cells due to inflammatory factors and the development of insulin resistance (6). Recently, researchers have demonstrated the relationship between mitochondrial dysfunction and insulin resistance, suggesting that mitochondrial dysfunction is significant in the pathogenesis and progression of T2DM (12). Previous studies have suggested that therapeutic modalities targeting mitochondria may effectively treat T2DM and its secondary defects (30,31). The present study aimed to investigate the role and mechanisms of genes associated with mitochondrial dysfunction in the risk prediction and progression of T2DM. Therefore, it combined bioinformatics analysis and experimental validation to investigate the role and mechanism of mitochondrial dysfunction-related genes in the prediction and development of T2DM risk.

First, the present study obtained five key genes associated with mitochondrial dysfunction in T2DM by bioinformatics analysis, including ERAP2, HLA-DQB1, HLA-DRB5, MAP1B and OAS3. It was demonstrated that ERAP2 played an important role in antigenic peptide processing, which is involved in the maturation of proteins in the endoplasmic reticulum and influences cytotoxic immune responses (32). ERAP2 was upregulated as a mitochondrial dysfunction-related gene in obstructive sleep apnea (33). HLA-DQB1 and HLA-DRB5 play an important role in the immune system by presenting peptides to T-cells and are differentially expressed in type 1 diabetes (34,35). The HLA-DQB1 allele is associated with T2DM and diabetic nephropathy in the Chinese Han population (36). MAP1B expression is associated with neurodevelopment and calcineurin-10 affects the progression of T2DM by regulating the cleavage of MAP1B (37,38). OAS3 expression is upregulated as a co-immunization biomarker in T2DM patients (39,40). The present study identified a significant downregulation of ERAP2 in T2DM, whereas the expressions of HLA-DQB1, HLA-DRB5, MAP1B and OAS3 were upregulated. In addition, MAP1B had an improved predictive performance for T2DM (AUC value of 0.759), whereas the AUC value was increased to 0.833 for the combined detection of the aforementioned five markers.

Addressing mitochondrial dysfunction could represent a novel therapeutic strategy for the management of T2DM (12). Pharmacological agents that enhance mitochondrial function, including specific antioxidants and mitochondrial protective compounds, may contribute to the restoration of normal metabolic processes, thereby improving insulin sensitivity

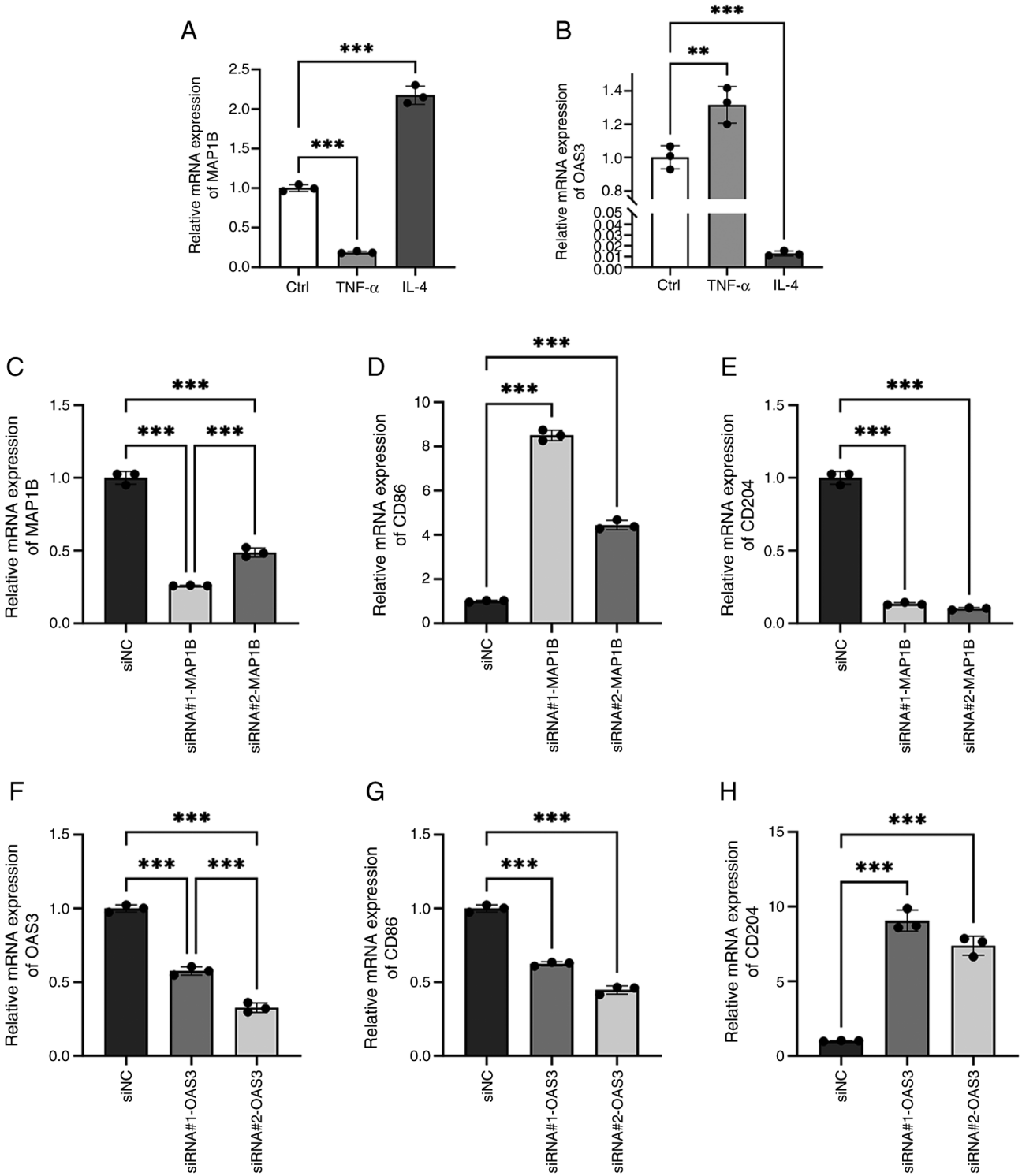

Figure 12. The effects of MAP1B and OAS3 on macrophage polarization. Detection of (A) MAP1B and (B) OAS3 n levels in TNF-α and IL-4 groups. RT-qPCR to detect the levels of (C) MAP1B, (D) CD86 and (E) CD204 following transfection of siRNA#1-MAP1B or siRNA#2-MAP1B. RT-qPCR to detect the expressions of (F) OAS3, (G) CD86 and (H) CD204 following transfection of siRNA#1-OAS3 or siRNA#2-OAS3; **P<0.01; ***P<0.001. MAPIB, microtubule-associated protein 1B; OAS3, 2'-5'-oligoadenylate synthetases; RT-qPCR, reverse transcription-quantitative PCR; siRNA, small interfering RNA; NC, negative control.

and glycemic regulation (12,41). The present study explored the potential role of these five markers (ERAP2, HLA-DQB1, HLA-DRB5, MAP1B and OAS3) in the treatment of T2DM and the results showed that these genes collectively target VPA. Turnbull *et al* (42) demonstrated a modest decrease in blood glucose levels in Wistar rats treated with VPA following administration of VPA, a result that was confirmed in subsequent preclinical studies (43-45). Several clinical studies also found lower blood glucose levels in VPA-treated patients (46,47). In the present study, molecular docking results showed that VPA was able to bind to the five markers (ERAP2, HLA-DQB1, HLA-DRB5, MAP1B and OAS3) through the

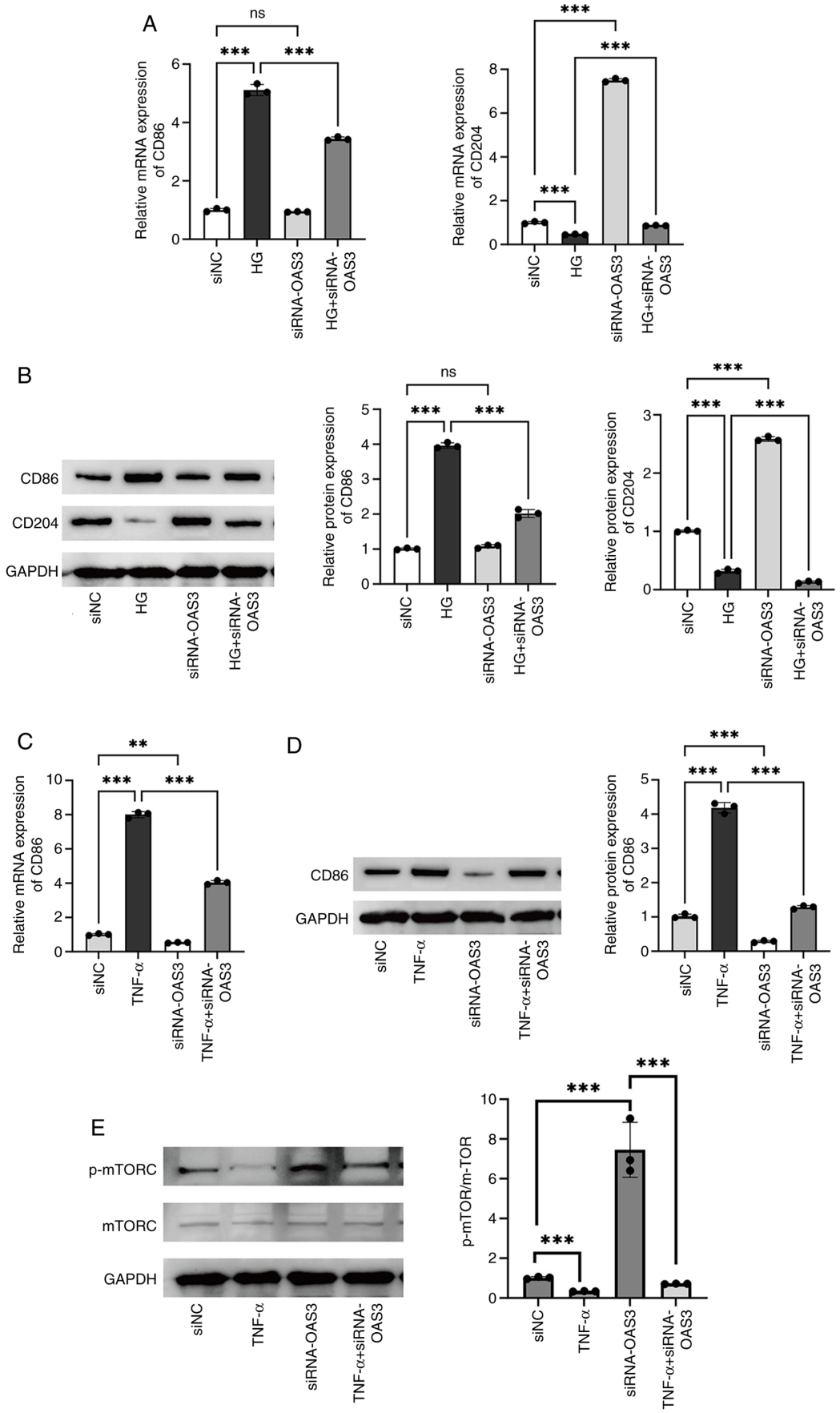

Figure 13. OAS3 modulates macrophage polarization markers (CD86/CD204) and mTOR signaling in type 2 diabetes mellitus models. (A) RT-qPCR to detect the levels of CD86 and CD204. (B) Western blotting to detect the protein expression levels of CD86 and CD204. (C) RT-qPCR to detect the expressions of CD86. (D) Western blotting to detect the protein expressions of CD86. (E) Protein expression levels of mTORC and p-mTORC were detected by western blotting; **P<0.01; ***P<0.001; ns: no significant difference. RT-qPCR, reverse transcription-quantitative PCR; siRNA, small interfering RNA; NC, negative control; MAPIB, microtubule-associated protein 1B; OAS3, 2'-5'-oligoadenylate synthetases; p-, phosphorylated.

formation of a stable hydrogen bond toward binding. The findings indicate that investigating mitochondrial dysfunction offers a potential target for the development of innovative therapeutic strategies. Furthermore, early identification and intervention in mitochondrial dysfunction may mitigate the risk of diabetic complications, thereby enhancing quality of life and prognosis in patients.

Metabolic disorders associated with T2DM are intricately linked to immune system function (48). The metabolic condition of mitochondria influences not only energy production but also modulates the activity and functionality of immune cells (48). Studies have shown that immune system disorders are closely related to the progression of T2DM (49). Accumulation of immune cells and inflammatory mediators in pancreatic islets, as well as immune cell infiltration, is one of the key features of islet dysfunction (50). Previous studies have demonstrated the effect of T cells on T2DM (51-53). $CD4^+$ T cells, as the main cells that make up the body's immune system, play a crucial role in the development of the disease. The helper T cells differentiated from $CD4^+$ T cells contain three subpopulations, Th1, Th2 and Th17 and serum TNF-α secreted by Th1 cells and IL-4, IL-10 secreted by Th2 cells, as well as IL-17 secreted by Th17 cells, have been shown to play an important role in the development of diabetes (54-56). $CD8^+$ T cells contribute to the development of chronic low-grade inflammation by secreting pro-inflammatory cytokines and expressing cytotoxic molecules (57,58). In addition, a number of studies have shown that macrophage infiltration is increased in pancreatic islets of T2DM patients (59-61). The present study found a significant decrease in the abundance of $CD4^+$ T cells and $CD8^+$ T cells and a substantial enrichment of macrophages in T2DM based on bioinformatics analysis. In addition, it found that $CD4^+$ T cells were notably associated with ERAP2, whereas $CD8^+$ T cells were notably associated with OAS3, MAP1B and ERAP2. Mitochondrial dysfunction is a critical factor in the pathogenesis of T2DM, notably influencing the immune microenvironment and thereby exacerbating insulin resistance and metabolic disorders. A comprehensive understanding of this intricate interaction is essential not only for elucidating the pathological mechanisms underlying T2DM but also for identifying potential targets for novel therapeutic strategies. Future research should further investigate the relationship between mitochondrial function and immune response to facilitate the development of more effective interventions for the management of T2DM.

Patients with T2DM develop an imbalance in macrophage M1/M2 polarization, which is manifested by an increase in pro-inflammatory M1 macrophages and a decrease in anti-inflammatory M2 macrophages (62). Chronic inflammation mediated by an imbalance in macrophage M1/M2 polarization may be a key factor in insulin resistance and pancreatic β-cell dysfunction (62). The present study revealed a significant increase in the expression of the M1 macrophage markers CD86, CD80 and CD68 and a decrease in the expression of the M2 macrophage markers CD204, CD206 and CD163 in a high-glucose environment. ERAP2, HLA-DQB1, HLA-DRB5, MAP1B and OAS3 are closely associated with immune responses and previous studies have reported their expression in macrophages (63-67). Since the murine sequences of ERAP2, HLA-DQB1 and HLA-DRB5 were not retrieved from the NCBI database, MAP1B and OAS3 were chosen for cellular experimental validation. One study notes that MAP1B could be used as a prognostic marker for bladder cancer patients and was notably positively correlated with the M2 macrophage-associated gene CD163 (66). Another study indicates that OAS3 was positively correlated with M1 macrophages in systemic lupus erythematosus (68). The present study showed that the expression of MAP1B and OAS3 was notably upregulated in HG-induced RAW264.7 cells and that the expression of MAP1B was higher in M2 macrophages. By contrast, the expression of OAS3 was higher in M1 macrophages. In addition, it was found that OAS3 showed activation in the mTORC1 signaling pathway by GSEA. A previous study confirmed that mTORC1 reduces insulin sensitivity by inhibiting insulin signaling (69). The present study found that downregulation of OAS3 expression attenuated M1 macrophage polarization by upregulating p-mTORC levels.

There are still some limitations to the present study. First, it obtained five biomarkers based on bioinformatics analysis, but since there were no mouse sequences for ERAP2, HLA-DQB1 and HLA-DRB5, Only MAP1B and OAS3 were experimentally validated. In addition, it was not experimentally demonstrated that VPA could target the expression of five biomarkers to alleviate the progression of T2DM. Future studies will conduct a more comprehensive analysis of the clinical application value and mechanism of action of the five biomarkers.

In conclusion, the present study screened five mitochondrial dysfunction biomarkers (ERAP2, HLA-DQB1, HLA-DRB5, MAP1B and OAS3) associated with T2DM and the combined detection of the aforementioned five markers has good efficacy in T2DM prediction. In addition, the aforementioned five marker genes may be target-regulated genes of VPA. Moreover, downregulation of OAS3 expression could attenuate the degree of M1 macrophage polarization by regulating the level of p-mTORC and thus regulate the progression of T2DM.

Acknowledgements

Not applicable.

Funding

No funding was received.

Availability of data and materials

The data generated in the present study may be requested from the corresponding author.

Authors' contributions

ML contributed to the conception and design. ML and HQ contributed to the collection and assembly of data. ML and HQ analyzed and interpreted the data. ML and HQ confirm the authenticity of all the raw data. Both authors read and approved the final version of the manuscript.

Ethics approval and consent to participate

Not applicable.

Patient consent for publication

Not applicable.

Competing interests

The authors declare that they have no competing interests.

References

1. Diane A, Allouch A, Mu UMRBA and Al-Siddiqi HH: Endoplasmic reticulum stress in pancreatic β-cell dysfunctionality and diabetes mellitus: A promising target for generation of functional hPSC-derived β-cells in vitro. Front Endocrinol (Lausanne) 15: 1386471, 2024.
2. Ding Y, Shi Y, Guan R, Yan S, Liu H, Wang Z, Li J, Wang T, Cai W and Ma G: Evaluation and comparison of efficacy and safety of tirzepatide and semaglutide in patients with type 2 diabetes mellitus: A Bayesian network meta-analysis. Pharmacol Res 199: 107031, 2024.
3. Ye H, Wang R, Wei J, Wang Y, Zhang X and Wang L: Bioinformatics analysis identifies potential ferroptosis key gene in type 2 diabetic islet dysfunction. Front Endocrinol (Lausanne) 13: 904312, 2022.
4. Zheng Y, Ley SH and Hu FB: Global aetiology and epidemiology of type 2 diabetes mellitus and its complications. Nat Rev Endocrinol 14: 88-98, 2018.
5. Sandoval DA and Patti ME: Glucose metabolism after bariatric surgery: Implications for T2DM remission and hypoglycaemia. Nat Rev Endocrinol 19: 164-176, 2023.
6. Ruze R, Liu T, Zou X, Song J, Chen Y, Xu R, Yin X and Xu Q: Obesity and type 2 diabetes mellitus: Connections in epidemiology, pathogenesis and treatments. Front Endocrinol (Lausanne) 14: 1161521, 2023.
7. Marin-Penalver JJ, Martin-Timon I, Sevillano-Collantes C and Del Canizo-Gomez FJ: Update on the treatment of type 2 diabetes mellitus. World J Diabetes 7: 354-395, 2016.
8. Ortiz-Martinez M, Gonzalez-Gonzalez M, Martagon AJ, Hlavinka V, Willson RC and Rito-Palomares M: Recent developments in biomarkers for diagnosis and screening of type 2 diabetes Mellitus. Curr Diab Rep 22: 95-115, 2022.
9. Rovira-Llopis S, Banuls C, Diaz-Morales N, Hernandez-Mijares A, Rocha M and Victor VM: Mitochondrial dynamics in type 2 diabetes: Pathophysiological implications. Redox Biol 11: 637-645, 2017.
10. Baker ZN, Forny P and Pagliarini DJ: Mitochondrial proteome research: The road ahead. Nat Rev Mol Cell Biol 25: 65-82, 2024.
11. Miwa S, Kashyap S, Chini E and von Zglinicki T: Mitochondrial dysfunction in cell senescence and aging. J Clin Invest 132: 2022.
12. Pinti MV, Fink GK, Hathaway QA, Durr AJ, Kunovac A and Hollander JM: Mitochondrial dysfunction in type 2 diabetes mellitus: An Organ-based analysis. Am J Physiol Endocrinol Metab 316: E268-E285, 2019.
13. Palma FR, Gantner BN, Sakiyama MJ, Kayzuka C, Shukla S, Lacchini R, Cunniff B and Bonini MG: ROS production by mitochondria: Function or dysfunction? Oncogene 43: 295-303, 2024.
14. Apostolova N, Vezza T, Muntane J, Rocha M and Victor VM: Mitochondrial dysfunction and mitophagy in type 2 diabetes: Pathophysiology and therapeutic targets. Antioxid Redox Signal 39: 278-320, 2023.
15. Shan Z, Fa WH, Tian CR, Yuan CS and Jie N: Mitophagy and mitochondrial dynamics in type 2 diabetes mellitus treatment. Aging (Albany NY) 14: 2902-2919, 2022.
16. Shen S, Liao Q, Wong YK, Chen X, Yang C, Xu C, Sun J and Wang J: The role of melatonin in the treatment of type 2 diabetes mellitus and Alzheimer's disease. Int J Biol Sci 18: 983-994, 2022.
17. Luo M, Zhao F, Cheng H, Su M and Wang Y: Macrophage polarization: An important role in inflammatory diseases. Front Immunol 15: 1352946, 2024.
18. Langfelder P and Horvath S: WGCNA: An R package for weighted correlation network analysis. BMC Bioinformatics 9: 559, 2008.
19. Xie W, Li J, Du H and Xia J: Causal relationship between PCSK9 inhibitor and autoimmune diseases: A drug target Mendelian randomization study. Arthritis Res Ther 25: 148, 2023.
20. Hemani G, Zheng J, Elsworth B, Wade KH, Haberland V, Baird D, Laurin C, Burgess S, Bowden J, Langdon R, *et al*: The MR-Base platform supports systematic causal inference across the human phenome. Elife 7: e34408, 2018.
21. Yang S, Guo J, Kong Z, Deng M, Da J, Lin X, Peng S, Fu J, Luo T, Ma J, *et al*: Causal effects of gut microbiota on sepsis and sepsis-related death: Insights from genome-wide Mendelian randomization, single-cell RNA, bulk RNA sequencing and network pharmacology. J Transl Med 22: 10, 2024.
22. Livak KJ and Schmittgen TD: Analysis of relative gene expression data using real-time quantitative PCR and the 2(-Delta Delta C(T)) method. Methods 25: 402-408, 2001.
23. Shen B, Liu J, Wu D, and Guo J: Evaluation of the safety and efficacy of high-dose rate brachytherapy for radiorecurrent prostate cancer: Asystematic review and meta-analysis. Strahlenther Onkol 200: 655-670, 2024.
24. Namazi N, Moghaddam SS, Esmaeili S, Peimani M, Tehrani YS, Bandarian F, Shobeiri P, Nasli-Esfahani E, Malekpour MR, Rezaei N, *et al*: Burden of type 2 diabetes mellitus and its risk factors in North Africa and the Middle East, 1990-2019: findings from the Global Burden of Disease study 2019. BMC Public Health 24: 98, 2024.
25. Huang X, He Y, Xu H, Shen Y, Pan X, Wu J and Chen K: Association between sociodemographic status and the T2DM-related risks in China: Implication for reducing T2DM disease burden. Front Public Health 11: 1297203, 2023.
26. Herman WH: Are There Clinical implications of racial differences in HbA1c? Yes, to not consider can do great harm! Diabetes Care 39: 1458-1461, 2016.
27. Alidrisi HA, Al-Ibadi AA, Al-Saidi JS, Alsawad MA, Jameel AA and Al-Shati AW: Comparative analysis of glycemic and lipid profiles in newly diagnosed males and females with type 2 diabetes mellitus. Cureus 15: e50101, 2023.
28. Parrinello CM and Selvin E: Beyond HbA1c and glucose: The role of nontraditional glycemic markers in diabetes diagnosis, prognosis and management. Curr Diab Rep 14: 548, 2014.
29. Xu H, Chen R, Hou X, Li N, Han Y and Ji S: The clinical potential of 1,5-anhydroglucitol as biomarker in diabetes mellitus. Front Endocrinol (Lausanne) 15: 1471577, 2024.
30. Blagov A, Nedosugova L, Kirichenko T, Sukhorukov V, Melnichenko A and Orekhov A: Mitochondrial dysfunction as a factor of energy metabolism disorders in type 2 diabetes mellitus. Front Biosci (Schol Ed) 16: 5, 2024.
31. Gao X, Yu X, Zhang C, Wang Y, Sun Y, Sun H, Zhang H, Shi Y and He X: Telomeres and mitochondrial metabolism: Implications for cellular senescence and Age-related diseases. Stem Cell Rev Rep 18: 2315-2327, 2022.
32. Mattorre B, Caristi S, Donato S, Volpe E, Faiella M, Paiardini A, Sorrentino R and Paladini F: A Short ERAP2 that binds IRAP is expressed in macrophages independently of gene variation. Int J Mol Sci 23: 4961, 2022.
33. Liu Q, Hao T, Li L, Huang D, Lin Z, Fang Y, Wang D and Zhang X: Construction of a mitochondrial dysfunction related signature of diagnosed model to obstructive sleep apnea. Front Genet 13: 1056691, 2022.
34. Anderson K, Carey B, Martin A, Roark C, Chalk C, Nowell-Bostic M, Freed B, Aubrey M, Trapnell B and Fontenot A: Pulmonary alveolar proteinosis: An autoimmune disease lacking an HLA association. PLoS One 14: e0213179, 2019.
35. Qiu YH, Deng FY, Tang ZX, Jiang ZH and Lei SF: Functional relevance for type 1 diabetes Mellitus-associated genetic variants by using integrative analyses. Hum Immunol 76: 753-758, 2015.
36. Ma ZJ, Sun P, Guo G, Zhang R and Chen LM: Association of the HLA-DQA1 and HLA-DQB1 alleles in type 2 diabetes mellitus and diabetic nephropathy in the han ethnicity of China. J Diabetes Res 2013: 452537, 2013.
37. Inoue H, Kanda T, Hayashi G, Munenaga R, Yoshida M, Hasegawa K, Miyagawa T, Kurumada Y, Hasegawa J, Wada T, *et al*: A MAP1B-cortactin-Tks5 axis regulates TNBC invasion and tumorigenesis. J Cell Biol 223: e202303102, 2024.
38. Hatta T, Iemura SI, Ohishi T, Nakayama H, Seimiya H, Yasuda T, Iizuka K, Fukuda M, Takeda J, Natsume T and Horikawa Y: Calpain-10 regulates actin dynamics by proteolysis of microtubule-associated protein 1B. Sci Rep 8: 16756, 2018.

39. Li XY, Hou L, Zhang LY, Zhang L, Wang D, Wang Z, Wen MZ and Yang XT: OAS3 is a Co-immune biomarker associated with tumour microenvironment, disease staging, prognosis and treatment response in multiple cancer types. Front Cell Dev Biol 10: 815480, 2022.
40. Wu C, Chen X, Shu J and Lee CT: Whole-genome expression analyses of type 2 diabetes in human skin reveal altered immune function and burden of infection. Oncotarget 8: 34601-34609, 2017.
41. Potenza MA, Sgarra L, Desantis V, Nacci C and Montagnani M: Diabetes and Alzheimer's Disease: Might mitochondrial dysfunction help deciphering the common path? Antioxidants (Basel) 10: 1257, 2021.
42. Turnbull DM, Bone AJ, Tames FJ, Wilson L, Baird JD and Sherratt HS: The effect of valproate on blood metabolite concentrations in spontaneously diabetic, ketoacidotic, BB/E Wistar rats. Diabetes Res 2: 45-48, 1985.
43. Kuretu A, Arineitwe C, Mothibe M, Ngubane P, Khathi A and Sibiya N: Drug-induced mitochondrial toxicity: Risks of developing glucose handling impairments. Front Endocrinol (Lausanne) 14: 1123928, 2023.
44. Stakisaitis D, Kapocius L, Kilimaite E, Gečys D, Šlekienė L, Balnytė I, Palubinskienė J and Lesauskaitė V: Preclinical study in mouse thymus and thymocytes: Effects of treatment with a combination of sodium dichloroacetate and sodium valproate on infectious inflammation pathways. Pharmaceutics 15: 2715, 2023.
45. Khan S and Jena G: Valproic acid improves glucose homeostasis by increasing beta-cell proliferation, function and reducing its apoptosis through HDAC inhibition in juvenile diabetic rat. J Biochem Mol Toxicol 30: 438-446, 2016.
46. Cicek NP, Kamasak T, Serin M, Okten A, Alver A and Cansu A: The effects of valproate and topiramate use on serum insulin, leptin, neuropeptide Y and ghrelin levels in epileptic children. Seizure 58: 90-95, 2018.
47. Tien N, Wu TY, Lin CL, Chu FY, Wang CCN, Hsu CY, Tsai FJ, Fang YJ and Lim YP: Association of epilepsy, anti-epileptic drugs (AEDs) and type 2 diabetes mellitus (T2DM): A population-based cohort retrospective study, impact of AEDs on T2DM-related molecular pathway and via peroxisome proliferator-activated receptor gamma transactivation. Front Endocrinol (Lausanne) 14: 1156952, 2023.
48. Daryabor G, Atashzar MR, Kabelitz D, Meri S and Kalantar K: The effects of type 2 diabetes mellitus on organ metabolism and the immune system. Front Immunol 11: 1582, 2020.
49. Painter JD and Akbari O: Type 2 innate lymphoid cells: Protectors in type 2 Diabetes. Front Immunol 12: 727008, 2021.
50. Song Y, He C, Jiang Y, Yang M, Xu Z, Yuan L, Zhang W and Xu Y: Bulk and single-cell transcriptome analyses of islet tissue unravel gene signatures associated with pyroptosis and immune infiltration in type 2 diabetes. Front Endocrinol (Lausanne) 14: 1132194, 2023.
51. Zhang S, Gang X, Yang S, Cui M, Sun L, Li Z and Wang G: The alterations in and the role of the Th17/Treg balance in metabolic diseases. Front Immunol 12: 678355, 2021.
52. Xia C, Rao X and Zhong J: Role of T lymphocytes in type 2 diabetes and diabetes-associated inflammation. J Diabetes Res 2017: 6494795, 2017.
53. Sun Q, Yang P, Gu QW, Gu WS, Wang W, Wang J and Mao XM: Increased glycemic variability results in abnormal differentiation of T cell subpopulation in type 2 diabetes patients. J Diabetes Complications 38: 108738, 2024.
54. Abdel-Moneim A, Bakery HH and Allam G: The potential pathogenic role of IL-17/Th17 cells in both type 1 and type 2 diabetes mellitus. Biomed Pharmacother 101: 287-292, 2018.
55. Wang C and Zhou B: Associations of blood glucose, helper T cells and cytokine levels with degree of periodontal lesion in type 2 diabetes mellitus patients accompanied by chronic periodontitis. Afr Health Sci 23: 239-245, 2023.
56. Ju SH, Lim JY, Song M, Kim JM, Kang YE, Yi HS, Joung KH, Lee JH, Kim HJ and Ku BJ: Distinct effects of rosuvastatin and rosuvastatin/ezetimibe on senescence markers of CD8+ T cells in patients with type 2 diabetes mellitus: A randomized controlled trial. Front Endocrinol (Lausanne) 15: 1336357, 2024.
57. Ju SH and Ku BJ: Effects of rosuvastatin/ezetimibe on senescence of CD8+ T-cell in type 2 diabetic patients with hypercholesterolemia: A study protocol. Medicine (Baltimore) 101: e31691, 2022.
58. Osawa Y, Studenski SA and Ferrucci L: Knee extension rate of velocity development affects walking performance differently in men and women. Exp Gerontol 112: 63-67, 2018.
59. Gao D, Jiao J, Wang Z, Huang X, Ni X, Fang S, Zhou Q, Zhu X, Sun L, Yang Z and Yuan H: The roles of cell-cell and organ-organ crosstalk in the type 2 diabetes mellitus associated inflammatory microenvironment. Cytokine Growth Factor Rev 66: 15-25, 2022.
60. Lee MK, Ryu H, Van JY, Kim MJ, Jeong HH, Jung WK, Jun JY and Lee B: The role of macrophage populations in skeletal muscle insulin sensitivity: Current understanding and implications. Int J Mol Sci 24: 11467, 2023.
61. Pivari F, Mingione A, Brasacchio C and Soldati L: Curcumin and Type 2 Diabetes Mellitus: Prevention and Treatment. Nutrients 11: 1837, 2019.
62. Banu S and Sur D: Role of macrophage in type 2 diabetes mellitus: macrophage polarization a new paradigm for treatment of type 2 diabetes mellitus. Endocr Metab Immune Disord Drug Targets 23: 2-11, 2023.
63. Schachinger E, Chanda G, Lobo RP, Naito M and Pronin AV: Eliashberg analysis of the optical conductivity in superconducting Pr2CuOx with x ≃ 4. J Phys Condens Matter 27: 045702, 2015.
64. Zhang JA, Zhou XY, Huang D, Luan C, Gu H, Ju M and Chen K: Development of an Immune-related gene signature for prognosis in melanoma. Front Oncol 10: 602555, 2020.
65. O'Brien CL, Summers KM, Martin NM, Carter-Cusack D, Yang Y, Barua R, Dixit OVA, Hume DA and Pavli P: The relationship between extreme inter-individual variation in macrophage gene expression and genetic susceptibility to inflammatory bowel disease. Hum Genet 143: 233-261, 2024.
66. Lyu X, Qiang Y, Zhang B, Xu W, Cui Y and Ma L: Identification of immuno-infiltrating MAP1A as a prognosis-related biomarker for bladder cancer and its ceRNA network construction. Front Oncol 12: 1016542, 2022.
67. Monti A, Lopez-Serrano J, Prieto A and Nicasio MC: Broad-scope amination of aryl sulfamates catalyzed by a palladium phosphine complex. ACS Catal 13: 10945-10952, 2023.
68. Han Y, Liu S, Shi S, Shu Y, Lu C and Gu X: Screening of genes associated with immune infiltration of discoid lupus erythematosus based on weighted gene Co-expression network analysis. Biochem Genet 63: 465-482, 2025.
69. Khalid M, Alkaabi J, Khan MAB and Adem A: Insulin signal transduction perturbations in insulin resistance. Int J Mol Sci 22: 8590, 2021.